DOCKETED	
Docket Number:	25-OPT-02
Project Title:	Prairie Song Reliability Project
TN #:	265681
Document Title:	Attachments 1-7 to SORT Comment Letter
Description:	N/A
Filer:	System
Organization:	Jacqueline Ayer
Submitter Role:	Public
Submission Date:	8/18/2025 8:33:52 PM
Docketed Date:	8/19/2025

Comment Received From: Jacqueline Ayer

Submitted On: 8/18/2025 Docket Number: 25-OPT-02

Attachments 1-7 to SORT Comment Letter

Additional submitted attachment is included below.

ATTACHMENT 1
INTERPRETATION MEMORANDUM NO.
2012-03 ISSUED BY THE LOS ANGELES
COUNTY DEPARTMENT OF REGIONAL
PLANNING.



Los Angeles County Department of Regional Planning

A REGIONAL THE

Planning for the Challenges Ahead

Amy J. Bodek, AICP
Director of Regional Planning

Dennis SlavinChief Deputy Director,
Regional Planning

October 18, 2021

TO: Staff

FROM: Amy J. Bodek, AICP

Director of Regional Planning

SUBDIVISION AND ZONING ORDINANCE INTERPRETATION NO. 2021-03 - BATTERY ELECTRIC STORAGE SYSTEMS

PURPOSE

This memorandum provides an official interpretation of the Department of Regional Planning regarding the definition of utility-scale energy storage devices (Energy Storage Devices). This memorandum is intended to serve as interim guidance for staff until such interpretation is superseded by subsequent interpretations or is incorporated into Title 22 (Planning and Zoning) of the the Los Angeles County Code (County Code).

<u>APPLICABILITY</u>

This memorandum is applicable to all parcels within unincorporated Los Angeles County and is effective as of the date of this memo.

INTERPRETATION

County Code Section 22.14.050 defines "Electric Distribution Substation (EDS)" and "Electric Transmission Substation (ETS)." The primary difference between these uses pertains to the conveyance of energy to users, with ETS typically being larger in volume than EDS. For purposes of defining energy storage devices as a land use, energy storage devices shall be considered most similar to EDS.

BACKGROUND

With the recent growth in renewable energy production, particularly utility-scale solar and wind resources, there has been an increased need in the development and deployment

Subdivision and Zoning Ordinance Interpretation No. 2021-03 – Battery Electric Storage Systems
October 18, 2021
Page 2

of Battery Electric Storage Systems (BESS). These devices are essentially large battery systems with appurtenant equipment that store energy typically produced by renewable energy sources such as sunlight or wind. This energy is then released to the electrical grid during evening or peak periods, and can help even out imbalances that occur between the production and consumption of renewable energy.

BESS devices are similar in size, bulk, and use to EDS. These utility-like devices are typically comprised of 40-foot-by-8-foot steel containers on concrete pads to house battery systems, pad-mounted transformers, and switchgear.

JUSTIFICATION

EDS are allowed in all zones with either a Site Plan Review (SPR) or a Conditional Use Permit (CUP), except the Mixed Use Development Zone where it is prohibited. ETS are allowed only in commercial and industrial zones with a CUP and SPR respectively and in Open Space and Watershed Zones with an SPR. Unlike the conduit nature of transmission substations, BESS are more similar to EDS.

In conclusion, to regulate these facilities in a consistent manner and to properly regulate them for community compatibility, the use most closely associated with them shall be EDS. Development standards for EDSs, Section 22.140.200, shall apply to BESS.

AJB:DJD:MG:SD:lm

C: Starr Coleman, Assistant County Counsel
Elaine Lemke, Assistant County Counsel/Chief Advisor

K_CP_10132021_SUB_ZONING_ORDINANCE_INTERPRE_NO_2021-03_BATTERY_ELLECTRIC_STORAGE_SYSTEMS

ATTACHMENT 2 SORT'S ASSESSMENT OF THE DEVELOPER'S AV AREA PLAN CONFORMITY ANALYSIS (TABLE 3.6-1).

Table 1 AV Plan Policies that are Controverted by the BESS Project.

Policy LU 3.2: Except within economic Developer claims consistency simply because the BESS opportunity areas, limit the amount of Project does not have residential uses. However, the potential development in Very High BESS Project controverts this policy because it is a high Fire Hazard Severity Zones, through density development in a Very High Fire Hazard appropriate land use designations with Severity Zone that poses a significant wildfire risk very low residential densities, as because it is prone to fire, explosion, and deflagration. indicated in the Land Use Policy Map (Map 2.1) of this Area Plan. Policy LU 3.3: Except within economic Developer claims consistency because the BESS Project opportunity areas, limit the amount of does not have residential uses. However, the BESS potential development in Flood Zones Project involves non-residential development designated by the Federal Emergency (specifically, a 500 kV transmission line) in a FEMA-Management Agency, through designated Flood Zone; this makes it facially inconsistent with Policy LU 3.3 which only recognizes appropriate land use designations with very low residential densities, as low density residential uses as appropriate uses in indicated in the Land Use Policy Map FEMA Flood Zones. (Map 2.1) of this Area Plan. Policy LU 4.1: Direct the majority of Developer claims consistency because the BESS Project the unincorporated Antelope Valley's is remotely operated (a characteristic that is not future growth to the economic relevant). However, the BESS Project entirely opportunity areas and areas that are controverts this policy because it places a high density, served by existing or planned high intensity industrial development in an area with **no** infrastructure, public facilities, and infrastructure, public facilities, or public water systems. public water systems, as indicated in The project site has no public water or sewer the Land Use designations shown on connections and is nowhere near such infrastructure: the Land Use Policy Map (Map 2.1) of therefore, the Developer's claim that the BESS Project comports with this land use policy is unfounded. this Area Plan. Policy LU 5.1: Ensure that Developer claims consistency because the BESS Project development is consistent with the helps achieve Renewable Portfolio Standards (RPS) goals. However, this policy pertains to the Sustainable Sustainable Communities Strategy adopted in 2012, an element of the Communities Strategy which is entirely unrelated to Regional Transportation Plan (and in fact does not even mention) RPS goals⁹². The developed by the Southern California BESS Project does not comport with this land use policy. Association of Governments. Policy LU 6.2: Ensure that the Area Developer claims consistency because the BESS Project Plan is flexible in adapting to new "supports the local community" by improving grid issues and opportunities without reliability. However, the BESS Project does not improve compromising the rural character of electrical service to the local community and it the unincorporated Antelope Valley. controverts this policy because it substantially compromises the rural character of Acton with the development of an impermissible industrial

development near multiple designated scenic drives⁹³.

⁹² The Sustainable Communities Strategy can be found here:

https://libraryarchives.metro.net/dpgtl/scag/2012-2035-regional-transportation-plan.pdf

⁹³ As indicated in Map 4.2 adopted with the AV Area Plan, the high density industrial BESS Project is located near the following designated scenic drives: Soledad Canyon Road, the Angeles Forest Highway, Aliso Canyon Road, and the 14 Freeway.

Policy COS 3.1: Discourage the use of chemical fertilizers, herbicides and pesticides in landscaping to reduce water pollution.	Developer claims consistency because the BESS Project commits to limiting chemical use "to the extent feasible" however the BESS project controverts this policy because it will substantially increase chemical usage in a natural area where chemicals are not currently used.	
Policy COS 3.2: Restrict the use of septic systems in areas adjacent to aqueducts and waterways to prevent wastewater intrusion into the water supply.	Developer claims consistency because the BESS Project will include the construction of a septic system; however, this policy does not apply because the BESS Project is not near a water supply source.	
Policy COS 3.4: Support preservation, restoration and strategic acquisition of open space to preserve natural streams, drainage channels, wetlands, and rivers, which are necessary for the healthy functioning of ecosystems.	Developer claims consistency because the Project will be decommissioned. However, the BESS Project substantially controverts this policy because it eliminates a massive open space area and does not acquire, preserve, or restore any streams, drainage channels, wetlands or rivers.	
Policy COS 3.5: Protect underground water supplies by enforcing controls on sources of pollutants.	Developer claims consistency because the BESS Project complies with adopted standards. However, the BESS Project actually threatens groundwater because it is susceptible to deflagration and the release of heavy metals.	
Policy COS 4.1: Direct the majority of the unincorporated Antelope Valley's future growth to rural town centers and economic opportunity areas, minimizing the potential for habitat loss and negative impacts in Significant Ecological Areas.	Developer claims consistency because the BESS Project is not in an SEA and because the transmission line "falls in line" with the Vincent Substation. However, the BESS Project transmission line is in, and will negatively impact, a Significant Ecological Area, so it clearly controverts Policy COS 4.1.	
Policy COS 4.2: Limit the amount of potential development in Significant Ecological Areas, including the Joshua Tree Woodlands, wildlife corridors, and other sensitive habitat areas, through appropriate land use designations with very low residential densities, as indicated in the Land Use Policy Map (Map 2.1) of this Area Plan.	Developer claims consistency because the BESS Project "limits the amount of disturbance" in an SEA. However, the BESS Project creates an industrial, 243 foot high non-residential development in an SEA, so it is intrinsically inconsistent with Policy COS 4.2. Equally important, the BESS project threatens the SEA with its ignition prone BESS units and a long transmission line that is susceptible to sparking a wildfire.	
Policy COS 4.3: Require new development in Significant Ecological Areas to comply with applicable Zoning Code requirements, ensuring that development occurs on the most environmentally suitable portions of the land and Policy COS 4.4: Require new development in Significant Ecological Areas, to consider certain design parameters.	Developer claims consistency because the 500 kV transmission line will comply with zoning requirements and because the project will include and stormwater facilities that "prevent erosion". However, the transmission line is not a permitted use in agricultural zones ⁹⁴ , so it does not comply with the zoning code. Additionally, the stormwater facilities are not in, or connected to, a Significant Ecological Areas; therefore, they are not relevant and do not demonstrate compliance with, these policies.	

 $^{^{94}}$ The Zoning Code does not allow private transmission lines in agricultural zones; it only allows transmission lines that are "publicly owned".

Policy COS 4.5: Subject to local, state or federal laws, require new development to provide adequate buffers from preserves, sanctuaries, habitat areas, wildlife corridors, State Parks, and National Forest lands, except within Economic Opportunity Areas.	Developer claims consistency because the BESS is not in an SEA, the 500 kV transmission line complies with Zoning, and the National Forest is more than 1 mile from the Project site. However, the transmission line <i>is</i> in an SEA and it <i>does not</i> comply with the Zoning Code. Furthermore, the BESS facility eliminates more than 70 acres of open space habitat area and has NO buffer for the adjacent SEA. The BESS Project directly controverts Policy COS 4.5.	
Policy COS 4.6: Encourage connections between natural open space areas to allow for wildlife movement and Policy COS 4.7: Restrict fencing in wildlife corridors.	Developer claims consistency because the BESS Project is located between two transportation corridors. However, the BESS Project provides no wildlife connections ⁹⁵ and therefore does not comply with either of these policies	
Policy COS 4.8: Ensure ongoing habitat preservation by coordinating with California Fish and Wildlife to obtain information on threatened and endangered species.	Developer claims consistency because communications with Fish and Wildlife have occurred. However, the BESS Project <i>does not</i> "ensure ongoing habitat preservation" because it destroys 70+ acres of habitat. Conversing with officials does not constitute consistency with this policy.	
Policy COS 4.9: Ensure water bodies are well-maintained to protect habitat areas and provide water to local specie; Policy COS 4.10: Restrict development that would reduce size of water bodies and minimize potential for loss of habitat and water supply.	Developer claims consistency, but Policies 4.9 and 4.10 are not applicable because the BESS Project does not involve a "water body". However, the BESS Project does destroy an extensive habitat area adjacent to the Santa Clara River headwaters, it its propensity for deflagration does threaten habitat in the Santa Clara River, so the BESS Project actually controverts these policies.	
Policy COS 5.7: Ensure that incompatible development is discouraged in designated Scenic Drives by developing and implementing development standards and guidelines for development within identified viewsheds of these routes (Map 4.2: Antelope Valley Scenic Drives).	Developer claims this policy is irrelevant because the BESS Project site "is not in a designated Scenic Drive". This is a gross misrepresentation of this Policy (which pertains to <i>viewsheds</i> of scenic drives). The BESS Project is located between 2 scenic drives and is in the viewshed of both; therefore, this policy clearly applies. The BESS Project also completely destroys these viewsheds; thus, it definitively and substantially controverts this policy.	
Policy COS 9.1: Implement land use patterns that reduce vehicle trips and air pollution;	Developer claims consistency because the BESS Project is "remotely operated" with only 16 workers. However, does not implement any land use patters, so Policy COS 9.1 is not particularly applicable	
Policy COS 9.2: Develop multi-modal transport systems that offer alternatives to auto travel to reduce vehicle trips, including regional transportation, transit, bicycle routes, trails, and pedestrian networks;	Developer claims consistency because the BESS Project is "remotely operated" with only 16 workers. However, the BESS Project does not offer a multi modal transport system and it actually <i>reduces</i> trail and pedestrian networks by <i>eliminating</i> existing trails and therefore does not comply.	

⁹⁵ The BESS Project is not in or near a wildlife linkage according to the "South Coast Missing Linkages" Study found here: http://www.scwildlands.org/reports/scmlregionalreport.pdf (pages 15-16).

Policy COS 9.3: In evaluating new development proposals, consider requiring trip reduction measures to relieve congestion and reduce air pollution from vehicle emissions.	Developer claims consistency because the BESS Project is "remotely operated" with only 16 workers. However, the Application presents no "trip reduction measures" for the 16 workers and thus does not comply	
Policy COS 9.7: Encourage reforestation and the planting of trees to sequester greenhouse gas emissions.	Developer claims consistency because there is a "Landscaping Plan" but the BESS Project "deforests" 70+ acres of native vegetation and SORT predicts that low shrubs and not trees will be planted (because of ignition risk).	
Policy COS 10.1: Encourage the use of non-hazardous materials in all utility-scale renewable energy production facilities to prevent the leaching of potentially dangerous run-off materials into the soil and watershed.	Developer claims consistency because the BESS Project will "implement procedures". However, the BESS Project substantially controverts this policy because the BESS units will consist of thousands of tons of hazardous materials that will release hazardous materials into the air and soil every time deflagration occurs.	
Policy COS 13.1: Direct utility-scale renewable energy production facilities, such as solar facilities, to locations where environmental, noise, and visual impacts will be minimized.	Developer claims consistency because the BESS Project is "on vacant land between two transportation corridors". However, the BESS Project is not in a location where environmental impacts are minimized, so it violates Policy COS 13.1 because of the noise, aesthetic, and public safety impacts it creates.	
Policy COS 13.3: Require all utility-scale renewable energy production facilities to develop and implement a decommissioning plan, with full and appropriate financial guarantee instruments that will restore the full site to its natural state upon complete discontinuance of operations and will restore non-operational portions of the site while the remainder continues operating.	Developer claims consistency because the BESS Project will "undergo decommissioning". However, the Application indicates the site will not be restored to its "natural state" upon decommissioning because Section 3.14 does not report that concrete waste will be generated during decommissioning even though the substation will have concrete foundations at least 7 feet deep and each BESS unit will have a concrete "slab on grade". Also, the "Decommissioning Plan" suggests footings will be "abandoned in place". Foundations that remain on site will impair native vegetation growth and preclude the return to a "natural state".	
Policy COS 13.5: Where utility-scale energy facilities cannot avoid sensitive biotic areas, require open space dedication in SEAs.	Developer claims consistency because the BESS Project "will comply" but the Application does not identify the size of the open space dedication or where it will be located (it merely states that "up to" 71 acres will be set aside).	
Policy COS 13.6: Ensure utility-scale renewable energy production facilities do not create land use conflicts with adjacent agricultural lands or existing residential areas. Require buffering and appropriate development standards to minimize potential conflicts; and Policy COS 13.7: Limit aesthetic impacts of utility-scale energy facilities to preserve rural character.	Developer claims consistency because the BESS Project will have an 8+ foot tan block wall that will "exhibit rural character". However, "BESS" is not a permitted land use; thus, the BESS Project intrinsically conflicts with adjacent agricultural lands. And, because it is impossible to configure a solid block wall to exhibit "rural character", the Acton Community Standards District prohibits solid perimeter walls because they are the <i>antithesis</i> of "rural character". The BESS Project will not comply with these policies.	

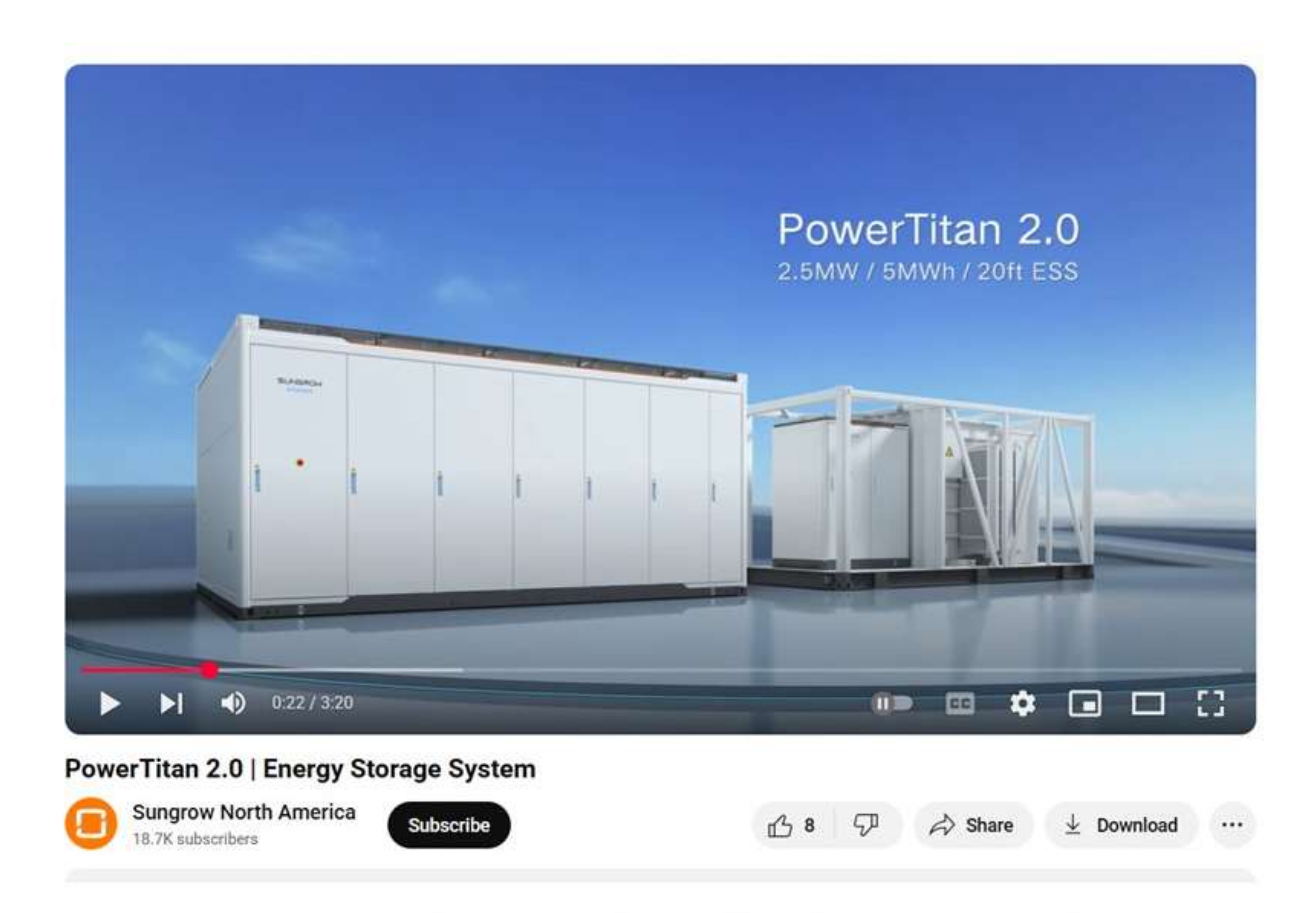
Policy COS 14.1: Require that new transmission lines be place underground whenever physically feasible.	Developer claims consistency however the BESS Project 500 kV transmission line will be constructed above ground.	
Policy COS 14.2: If new transmission lines cannot feasibly be placed underground due to physical constraints, require that they be collocated with existing transmission lines, or along existing transmission corridors, whenever physically feasible.	Developer claims consistency however the BESS Project 500 kV transmission line will not utilize an existing transmission corridor and instead will cut a new transmission corridor and access roads through sensitive biological resources in the Santa Clara River SEA	
Policy COS 14.3: If new transmission lines cannot be feasibly be placed underground or feasibly collocated with existing transmission lines or along existing transmission corridors due to physical constraints, direct new transmission lines to locations where visual and environmental impacts will be minimized.	Developer claims consistency however the BESS Project 500 kV transmission line will be constructed entirely within an SEA in a Very High Fire Hazard Severity Zone and with 243 foot high towers. Therefore, it will result in significant visual and environmental impacts that cannot be mitigated or minimized.	
Policy COS 14.4: Discourage the placement of new transmission lines on undisturbed lands containing sensitive biotic communities; Policy	Developer claims consistency however the BESS Project 500 kV transmission line will be constructed almost entirely on undisturbed land in an SEA that contains sensitive biotic communities	
Policy COS 14.5: Discourage placement of new transmission lines through existing communities or properties with existing residential uses.	Developer claims consistency however the BESS Project 500 kV transmission line will be located entirely within the existing community of locate on properties with existing residential uses.	
Policy COS 14.6: Review all proposed transmission line projects for conformity with the Goals and Policies of the AV Area Plan, including those listed above. When the California Public Utilities Commission is the decision-making authority for these projects, provide comments regarding conformity with the Goals and Policies of the Area Plan.	Developer claims consistency because the BESS Project will comply with CPUC General Orders and because the Application's Table 3.6-1 shows that the BESS Project is consistent with AV Plan policies. However, compliance with CPUC General Orders is irrelevant and it does not demonstrate consistency with AV Area Plan Goals and Policies. More importantly, the BESS Project transmission line controverts every single AV Area Plan goal and policy that applies to it; therefore, the BESS Project does not comport with Policy COS 14.6.	
Policy COS 16.1: Except within Economic Opportunity Areas, require development to minimize removal of native vegetation. Discourage clear- scraping of land and ensure a large percentage of land is left in its natural state.	Developer claims consistency because the BESS Project removes vegetation "to allow for fire protection and defensible space". The developer fails to grasp that this policy is intended to <i>preserve</i> native vegetation, not remove it. The BESS project <i>clear scrapes</i> all native vegetation from 70+ acres and leaves <i>nothing</i> in its natural state. It does not comport with Policy COS 16.1.	
Policy PS 1.2: Require new developments provide sufficient access for emergency vehicles and sufficient evacuation routes for residents and animals.	Developer claims consistency because the BESS Project will have internal roadways. However, this policy also pertains to access routes outside development. The BESS Project eliminates a secondary access route and thus does not comply	

_ 11	_ , ,,	
Policy PS 3.1: Limit the amount of potential development in Flood Zones designated by the Federal Emergency Management Agency through appropriate land use designations with very low residential densities.	Developer claims this policy is not applicable because the BESS Project "is not within a Flood Zone designated by the Federal Emergency Management Agency". However, the BESS Transmission Line <i>is</i> in a Flood Zone (Figure 3.15-41), and because it does not have a "very low residential density", it does not comply.	
Policy PS 3.2: Require onsite stormwater filtration in new developments through use of appropriate measures, such as permeable surface coverage, permeable paving of parking and pedestrian areas, catch basins, and other low impact development strategies.	Developer claims consistency because the BESS Project will include large stormwater facilities. The intent of this policy is to reduce dependencies on large stormwater facilities by using distributed "low impact" infiltration strategies (i.e. permeable surfaces and not hardscapes) in new developments. The BESS Project does not comport with this policy because it covers large areas with impermeable concrete pads, not "low impact" permeable surfaces.	
Policy ED 1.10: Promote small-scale, household based renewable energy systems to enable Antelope Valley residents to become energy independent.	Developer claims this policy is not applicable because the BESS Project is utility scale. However, utility scale energy projects like the BESS Project substantially controvert this policy by disincentivizing household based energy projects. This is because California now compels all customers to pay a fixed fee on their electrical bill to cover the cost of utility scale projects (like the BESS Project) even though customers with household-based renewable energy systems do not use power from such projects. The BESS Project controverts Policy ED 1.10 because it does not support small-scale, household based renewable energy systems; to the contrary, it disincentivizes them	
Policy ED 1.11: Encourage the development of utility-scale renewable energy projects at appropriate locations and with appropriate standards to ensure any negative impacts to local residents are sufficiently mitigated.	Developer claims consistency because the BESS Project avoids impacts to local residents since it is between two transportation corridors near the Vincent Substation. However, the BESS Project facially violates this policy because it is in a location that will create significant aesthetic, noise, public safety, and economic impacts on local residents <i>which cannot be mitigated</i> .	
Policy ED 1.12: Adopt regulations that ensure that local residents receive a fair share of the benefits of utility-scale renewable energy projects that are commensurate to their impacts.	Developer claims consistency because the BESS Project improves reliability on Acton's electrical grid and provides local jobs and tax revenues that benefit the community. This is incorrect. The BESS Project is not a renewable project and it will not improve reliability on Acton's grid because it is not connected to Acton's grid. It will not provide local jobs because union workers supplied by LAOCBCTC will come from Palmdale, Lancaster, and Santa Clarita. Tax revenues will not go to Acton, they will go into the County General Fund to support County priorities. Accordingly, if Policy ED 1.12 did apply, the BESS Project would violate it.	

Table 2. AV Plan Policies That are Omitted from the Application and Which are Controverted by the BESS Project.

Page LU-9: The intent and purpose of the "Rural" Land Use designation is to provide for "Single-family residences; equestrian and limited animal uses; and limited agricultural and related activities".	The BESS Project is not consistent with the intent and purpose of the "Rural" Land Use designation because it is not a single-family residence or an equestrian/limited animal use and it does not support a limited agricultural or related activity.
Page COMM-5: Various types of agricultural, equestrian, and animal keeping uses are allowed in Acton's Rural Town Areas provided Zoning Code requirements are met.	The BESS Project is located in Acton's Rural Town Area but it is not consistent with this land use policy because it is not an agricultural or equestrian or animal keeping use and it does not comply with the Zoning Code.

ATTACHMENT 3 TECHNICAL DATA FOR SUNGROW POWER TITAN II BESS UNITS.



Source: https://www.youtube.com/watch?v=kMMBLKe9jAo

ST5015UX-2H-US ST5015UX-4H-US

PowerTitan 2.0 Liquid Cooled Energy Storage System





- Intelligent liquid-cooled temperature control system to optimize the auxiliary power consumption
- Pre-assembled, no battery module handling on site, transportation of complete system

EFFICIENT AND FLEXIBLE

- High-efficiency heat dissipation, increase battery life and system discharge capacity
- Front single-door-open design, supporting back to back layout drawing
- Function test in factory, limited on-site work, accelerate commissioning process

(-<u></u><u></u><u></u><u></u><u></u>-<u></u>)

SAFE AND RELIABLE

- Electrical safety management, overcurrent fast breaking and arc extinguishing protection
- The electrical cabinet and battery cabinet are separated to prevent thermal runaway

CONVENIENT O&M

- · One-click system upgrade
- · Automatic coollant refilling design
- · Online intelligent monitoring





Product name	ST5015UX-2H-US	ST5015UX-4H-US	
DC side			
Cell type	LFP	LFP	
Cell type	3.2 V / 31	I4 Ah	
Battery configuration	416512	2P	
Nominal capacity	5015 k ^v	Wh	
Nominal voltage range	1123.2 V ~ 1	497.6 V	
AC side			
Nominal AC power	210 kVA * 12	210 kVA * 6	
AC current distortion rate	< 3 % (Nomin	nal Power)	
DC component	< 0.5	< 0.5 %	
Nominal AC voltage	690	V	
AC voltage range	607 V ~ '	759 V	
Termination (LV)	352 A * 3 Phase * 6	352 A * 3 Phase * 3	
Power factor	> 0.99 (Nomir	> 0.99 (Nominal Power)	
Adjustable range of reactive power	- 100 % ~ 100 %		
Nominal frequency	60 H	60 Hz	
Isolation method	Transformerless		
System parameter			
Dimension (W*H*D)	6058 mm * 2896 r	mm * 2438 mm	
Difficultion (W 11 D)	238.5'' * 114.0	238.5''* 114.0''* 96.0"	
Weight	42500 kg / 93696.5 lbs	42000 kg / 92594.0 lbs	
Degree of protection	Type 2	3S	
Anti-corrosion degree	C4		
Operation temperature range	-30 °C ~ 50 °C (>	-30 °C ~ 50 °C (> 45 °C Derating)	
operation temperature range	-22 °F ~ 122 °F (> 113 °F Derating)		
Operation humidity range		0 % ~ 100 %	
Max. operation altitude	3000 m/9	3000 m / 9842.5 ft	
Temperature control method	Intelligent Liqu	Intelligent Liquid Cooling	
	Default: NFPA 68 compliance vent panel,	Default: NFPA 68 compliance vent panel, smoke and heat, detectors, Mini FACP	
Fire suppression system	Optional: Sprinkler, sound beacon, NFPA 69, c	Optional: Sprinkler, sound beacon, NFPA 69, compliance ventilation system, Flammable	
	gas dete	ector	
Communication	Etherr	Ethernet	
Standard	UL 9540A, NFPA 855, NFPA	UL 9540A, NFPA 855, NFPA 68, NFPA 69 (optional)	
Standard	IEEE 1547, UL 1973, U	IL 1741SB, UL 9540	



ATTACHMENT 4 UNDERWRITERS LABORATORY PUBLICATION ON THE UL9540A CERTIFICATION PROCEDURE.



December 2, 2019

Authored by Howard D. Hopper, FPE - Global Regulatory Services Manager. Contributions by Adam Barowy, Research Engineer

In 2015 work began on developing fire safety requirements in U.S. fire codes to address modern energy storage systems (ESS). This effort focused on mitigating the potential hazards of large indoor and outdoor lithium-ion battery ESS installations. The greatest concern for ESS installations was thermal runaway in a battery module that could propagate to a significant fire or explosion, especially since there were no proven methods for controlling or suppressing a fire or mitigating a potential explosion. At the time there was a lack of research and fire performance data to use as a basis for developing protection solutions.

Size (electrical capacity in a unit), separation and maximum allowable quantity (total electrical capacity in one space) requirements were introduced in the 2018 International Fire Code and the NFPA 1 Fire Code to address uncertainty with thermal runaway and fire propagation of battery ESS. The size and electrical energy density of ESS installations were limited by these requirements. However, the codes allowed ESS installations with

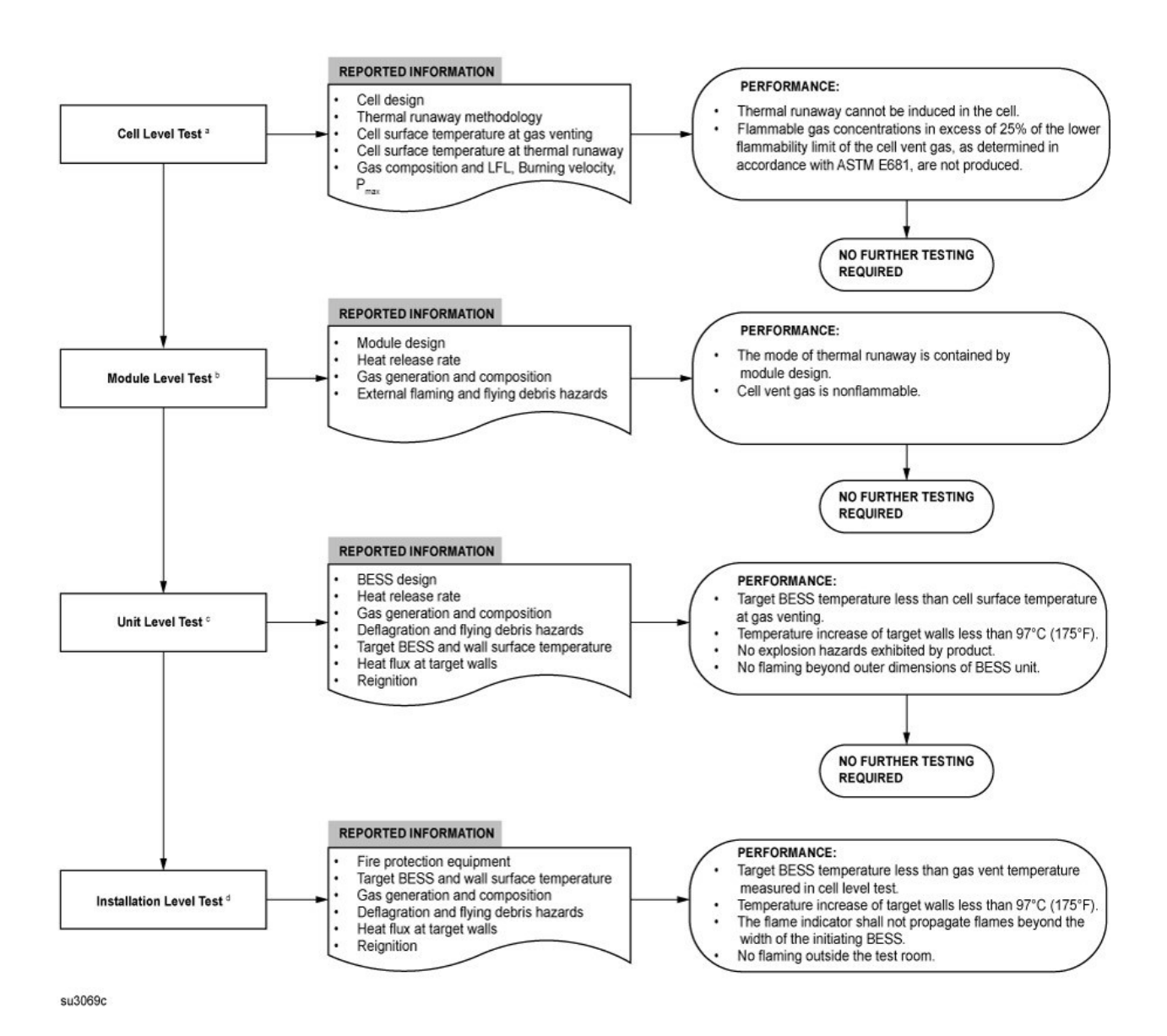
larger capacities or smaller separation distances when approved by the code authority using large-scale fire and fault condition testing results from an approved testing laboratory. This testing needed to demonstrate that a fire involving one ESS unit would not propagate to an adjacent unit and would be contained within a battery room.

UL stepped up to meet the needs of the ESS industry and code authorities by developing a methodology for conducting battery ESS fire tests by publishing UL 9540A¹, Test Method for Evaluating Thermal Runaway Fire Propagation in Battery Energy Storage Systems in November 2017. The requirements were designed to evaluate the fire characteristics of a battery ESS that undergoes thermal runaway. The data generated was intended to be used to determine the fire and explosion protection required for an installation of a battery energy storage system. It also meets the objectives of the International Fire Code (IFC) and NFPA 1 relative to fire propagation hazards and fire mitigation methods from a single battery energy storage system unit.

UL 9540A included a series of progressively larger fire tests, beginning at the cell level and progressing to the module level, unit level, and finally the installation level. Each test generated specific data used to evaluate thermal runaway characteristics and fire propagation without specific pass/fail test criteria. Instead, the complete data package was provided to code authorities so they could evaluate the suitability of a battery ESS installation.

As fire codes evolved, and UL gained additional experience with battery ESS fire propagation testing, thermal runaway characteristic, and the data needed by code authorities, UL 9540A was updated in rapid succession with a second edition published in January 2018 and a third edition published in June 2018. With the technical foundation for battery ESS large-scale fire testing firmly in place, UL engaged Standard Technical Panel 9540 in 2019 to develop a binational edition of the test method. The fourth edition of

ANSI/CAN/UL 9540A was published November 12, 2019 and is an ANSI and SCC (Standards Council of Canada) accredited standard.



A few of the significant changes introduced into the fourth edition of UL 9540A include:

 Criteria introduced to the cell level, module level, and unit level tests that identify when progressively larger tests are unnecessary,

- essentially establishing acceptance criteria for the tests. The flow chart accompanying this article provides details on the test sequence UL 9540A¹.
- Enhancements to the unit level test to include specific test criteria for testing indoor floor mounted battery energy storage systems (BESS), outdoor ground mounted BESS, indoor wall mounted BESS and outdoor wall mounted BESS. All of these types of systems are covered by specific installation requirements in the latest editions of the IFC, NFPA 1 and NFPA 855.

UL 9540A will continue to evolve to reflect changes in ESS installation requirements, advancements in fire science, and the needs of the ESS industry and code authorities. For additional information on UL 9540A, visit www.UL.com/batteries.

^{1.} Adapted from UL 9540A copyright © 2019 Underwriters Laboratories Inc.

ATTACHMENT 5 INCIDENT REPORT ON THE 2021 VICTORIA BESS FIRE INCIDENT.

Victorian Big Battery Fire: July 30, 2021

REPORT OF TECHNICAL FINDINGS

ANDY BLUM, PE, CFEI
SENIOR FIRE PROTECTION ENGINEER

Fisher Engineering, Inc.

10475 MEDLOCK BRIDGE ROAD SUITE 520 JOHNS CREEK GA 30097 TOM BENSEN, PRINCIPAL FOUNDER
PAUL ROGERS, PRINCIPAL FOUNDER
CASEY GRANT, PE, SENIOR CONSULTANT
GEORGE HOUGH, SENIOR CONSULTANT

Energy Safety Response Group 8350 US HIGHWAY N 23

DELAWARE OHIO 43015

Background

The Victorian Big Battery (VBB) is a 300-Megawatt (MW)/450-Megawatt hour (MWh) grid-scale battery storage project in Geelong, Australia. VBB is one of the largest battery installations in the world and can power over one million Victorian homes for 30 minutes during critical peak load situations.¹ It is designed to support the renewable energy industry by charging during times of excess renewable generation. The VBB is fitted with 212 Tesla Megapacks to provide the 300-MW/450-MWh of energy storage. The Megapack is a lithium-ion battery energy storage system (BESS) consisting of battery modules, power electronics, a thermal management system, and control systems all pre-manufactured within a single cabinet that is approximately 7.2 meters (m) in length, 1.6 m deep and 2.5 m in height (23.5 feet [ft] x 5.4 ft x 8.3 ft).

On Friday, July 30th, 2021, a single Megapack at VBB caught fire and spread to a neighboring Megapack during the initial installation and commissioning of the Megapacks. The fire did not spread beyond these two Megapacks and they burned themselves out over the course of approximately six hours. There were no injuries to the general public, to site personnel or to emergency first responders as the Megapacks failed safely (i.e., slowly burned themselves out with no explosions or deflagrations), as they are designed to do in the event of a fire. Per the guidance in Tesla's Lithium-Ion Battery Emergency Response Guide² (ERG), emergency responders permitted the Megapack to burn and consume itself while nearby exposures were being monitored at a safe distance. The total impact to the site was two out of the 212 Megapacks were fire damaged, or less than 1% of the BESS.

Following the emergency response, a detailed, multi-entity fire investigation commenced on August 3, 2021. The investigation process included local regulatory entities, Tesla, outside third-party engineers and subject matter experts. The investigation process involved analyzing both the fire origin and cause as well as the root cause of the fire propagation to the neighbor Megapack. In addition, given this is the first fire event in a Megapack installation to date, a review of the emergency response has been performed to identify any lessons learned from this fire event.

This report summarizes those investigations and analyses and has been prepared by Fisher Engineering, Inc. (FEI) and Energy Safety Response Group (ESRG), two independent engineering and energy storage fire safety consulting firms. In addition, this report provides a list of lessons learned from the fire and also highlights the procedural, software and hardware changes that have been implemented based on those lessons learned.

Incident Timeline

At the time of the fire, the VBB was fitted with approximately one-half of the 212 total Megapacks intended for the site. The Megapacks that were installed at VBB were undergoing routine testing and commissioning on the day of the fire. At 7:20 AM Australian Eastern Standard Time (AEST) on the morning of July 30, 2021, commissioning and testing of a number of Megapacks commenced. One such Megapack (denoted herein as MP-1), was not going to be tested that day and was therefore shut off manually by means of the keylock switch.³ At the time MP-1 was shut down via the keylock switch, the unit displayed no abnormal conditions to site personnel. Around 10:00 AM, smoke was observed emitting from MP-1 by site personnel. Site personnel

https://victorianbigbattery.com.au/

² https://www.tesla.com/sites/default/files/downloads/Lithium-lon Battery Emergency Response Guide en.pdf

³ The keylock switch is a type of "lock out tag out" switch on the front of the Megapack that safely powers down the unit for servicing.

electrically isolated all the Megapacks on-site and called emergency services: Country Fire Authority (CFA). The CFA arrived shortly thereafter and set up a 25 m (82 ft) perimeter around MP-1. They also began applying cooling water to nearby exposures as recommended in Tesla's ERG. The fire eventually spread into a neighbor Megapack (MP-2) installed 15 centimeters (cm), or 6 inches (in), behind MP-1. The CFA permitted MP-1 and MP-2 to burn themselves out and did not directly apply water into or onto either Megapack, as recommended in Tesla's ERG. By 4:00 PM (approximately six hours after the start of the event), visible fire had subdued and a fire watch was instituted. The CFA monitored the site for the next three days before deeming it under control on August 2, 2021, at which time, the CFA handed the site over for the fire investigation to begin.



Note: The time stamp is AEST (UTC+10) which is 19 hours ahead of USA PDT (UTC-7)

Investigation

A multi-entity fire investigation commenced on August 3, 2021. The VBB fire investigation process involved analyzing both the root cause of the initial fire in MP-1 as well as the root cause of the fire propagation into MP-2. The investigations included on-site inspections of MP-1 and MP-2 by the CFA, Energy Safe Victoria⁴ (ESV), Work Safety Victoria⁵ (WSV), local Tesla engineering/service teams and a local third-party independent engineering firm. In addition to the on-site work immediately after the incident, the root cause investigations also included data analysis, thermal modeling and physical testing (electrical and fire) performed by Tesla at their headquarters in California, USA and their fire test facility in Nevada, USA.

Fire Cause Investigation

On-site inspections commenced on August 3, 2021 and concluded on August 12, 2021. MP-1 and MP-2 were documented, inspected and preserved for future examinations, if necessary. Concurrently, all available telemetry data (such as internal temperatures and fault alarms) from MP-1 and MP-2 were analyzed and a series of electrical fault and fire tests were performed. The on-site investigation findings, the telemetry data analysis, electrical fault tests and fire tests, when combined, identified a very specific series of fault conditions present on July 30, 2021 that could lead to a fire event.

Fire Origin and Cause Determination

The origin of the fire was MP-1 and the most likely root cause of the fire was a leak within the liquid cooling system of MP-1 causing arcing in the power electronics of the Megapack's battery modules. This resulted in heating of the battery module's lithium-ion cells that led to a propagating thermal runaway event and the fire.

Other possible fire causes were considered during the fire cause investigation; however, the above sequence of events was the only fire cause scenario that fits all the evidence collected and analyzed to date.

Contributory Factors

A number of factors contributed to this incident. Had these contributory factors not been present, the initial fault condition would likely have been identified and interrupted (either manually or automatically) before it escalated into a fire event. These contributory factors include:

- 1. The supervisory control and data acquisition (SCADA) system for a Megapack required 24 hours to setup a connection for new equipment (i.e., a new Megapack) to provide full telemetry data functionality and remote monitoring by Tesla operators. Since VBB was still in the installation and commissioning phase of the project (i.e., not in operation), MP-1 had only been in service for 13 hours prior to being switched off via the keylock switch on the morning of the fire. As such, MP-1 had not been on-line for the required 24 hours, which prevented this unit from transmitting telemetry data (internal temperatures, fault alarms, etc.) to Tesla's off-site control facility on the morning of the fire.
- 2. The keylock switch for MP-1 was operated correctly on the morning of the fire to turn MP-1 off as the unit was not required for commissioning and testing that morning; however, this action caused telemetry systems, fault monitoring, and electrical fault safety devices⁶ to be disabled or operate with

Victoria's energy safety regulator

Victoria's health and safety regulator

These elements include, among other devices, fuses at the cell and module level for localized fault current interruption and a battery module pyro disconnect that severs the electrical connection of the battery module when a fault current is passing through the battery module.

- only limited functionality. This prevented some of the safety features of MP-1 from actively monitoring and interrupting the electrical fault conditions before escalating into a fire event.
- 3. The exposure of liquid coolant onto the battery modules likely disabled the power supply to the circuit that actuates the pyro disconnect.⁷ With a power supply failure, the pyro disconnect would not receive a signal to sever and would not be able to interrupt a fault current passing through the battery module prior to it escalating into a fire event.

Fire Propagation Investigation

The VBB fire investigation process involved analyzing not only the root cause of the initial fire in MP-1 but also the root cause of the fire propagation into MP-2. The Megapack has been designed to be installed in close proximity to each other without fire propagating to adjacent units. The design objective of the Megapack in terms of limiting fire propagation was mainly reliant on the thermal insulation of the Megapack's exterior vertical steel panels and the sheer mass of the battery modules acting as a heat sink (i.e., they are difficult to heat up). With this thermal insulation, the Megapack spacing can be as close as 15 cm (6 in) to the sides and back of each unit with 2.4 m (8 ft) aisles in front of each Megapack, as shown in Figure 1. This product spacing has been validated in UL9540A unit level tests.8 Similar to the fire origin and cause investigation, the on-site inspections were supported simultaneously with an analysis of telemetry data (such as internal temperatures) from MP-2 and fire testing. The on-site investigation findings, the telemetry data analysis and fire tests, when combined, identified a scenario where Megapack to Megapack fire propagation can occur.





Figure 1 VBB Megapack layout (top) and area of fire origin (bottom)

Report of Technical Findings: Victorian Big Battery Fire

The pyro disconnect is a Tesla proprietary shunt-controlled pyrotechnic fuse that allows for rapid one-time actuation. There is one pyro disconnect per battery module.

⁸ UL9540A, *Test Method for Evaluating Thermal Runaway Fire Propagation in Battery Energy Storage Systems*. UL9540A is a test method developed by UL to address fire safety concerns with BESS. The test method provides a method to evaluate thermal runaway and fire propagation at the cell level, module level, and unit level. In addition to cell and module level tests, Tesla performed unit level tests to evaluate, among other fire safety characteristics, the potential for fire propagation from Megapack-to-Megapack. During unit level testing, fire propagation did not occur between Megapacks when they were installed with a spacing of 15 cm (6 in) to the sides and back of each unit.

Fire Propagation Determination

Flames exiting the roof of MP-1 were significantly impacted by the wind conditions at the time of the fire. Wind speeds were recorded between 20-30 knots⁹ which pushed the flames exiting the roof of MP-1 towards the roof of MP-2. This direct flame impingement on the top of the thermal roof of MP-2 ignited the internal components of MP-2, most notably, the plastic overpressure vents that seal the battery bay¹⁰ from the thermal roof. Once ignited, the overpressure vents provided a direct path for flames and hot gases to enter into the battery bays, thus exposing the battery modules of MP-2 to fire and/or elevated temperatures. Exposed to temperatures above their thermal runaway threshold of 139°C (282°F), the cells within the battery modules eventually failed and became involved in the fire.

Other possible fire propagation root causes were considered during the investigation; however, the above sequence of events was the only fire propagation scenario that fits all the evidence collected and analyzed to date. Of note, at the time when fire was observed within the thermal roof of MP-2, internal cell temperature readings of MP-2 had only increased by 1°C (1.8°F) from 40°C to 41°C (104°F to 105.8°F)¹¹ Around the same time that fire was observed within the thermal roof of MP-2, around 11:57 AM (approximately 2 hours into the fire event), communication was lost to the unit and no additional telemetry data was transmitted. However, given the internal cell temperatures of MP-2 had only recorded a 1°C (1.8°F) temperature rise 2 hours into the fire event and while the unit's roof was actively on fire, fire propagation across the 15 cm (6 in) gap via heat transfer is not the root cause of the fire propagation. Furthermore, this telemetry data from MP-2 demonstrates that the Megapack's thermal insulation can provide significant thermal protection in the event of a fire within an adjacent Megapack installed only 15 cm (6 in) away.

Contributory Factors

The wind was the dominant contributory factor in the propagation of fire from MP-1 to MP-2. At the time of the fire, a 20-30 knot (37-56 km/hr, 23-35 mph) wind was recorded out of the north. The wind conditions at the time of the fire pushed the flames exiting out of the top of MP-1 towards the top of MP-2 leading to direct flame impingement on the thermal roof of MP-2. This type of flame behavior was not observed during previous product testing or regulatory testing per UL9540A. In UL9540A unit level testing, the maximum wind speed permitted during the test is 10.4 knots (19.3 km/hr, 12.0 mph); whereas, wind conditions during the VBB fire were two to three times greater in magnitude. As such, the wind conditions during the VBB fire appear to have identified a weakness in the Megapack's thermal roof design (unprotected, plastic overpressure vents in the ceiling of the battery bays) that allows Megapack-to-Megapack fire propagation. This weakness was not identified previously during product or regulatory testing and does not invalidate the Megapack's UL9540A certification, as the cause of fire propagation was primarily due to an environmental condition (wind) that is not captured in the UL9540A test method.

⁹ This equates to 37-56 kilometers per hour (km/hr) or 23-35 miles per hour (mph).

The battery bay is an IP66 enclosure that houses the battery modules. It is distinct from the thermal roof installed above it. Plastic overpressure vents are installed in the ceiling of the battery bay, sealing the two enclosures from one another.

As a reference, the Megapack's normal operating cell temperature is between 20-50°C and cell thermal runaway does not occur until 139°C (98°C above cell temperatures of MP-2 before telemetry data was lost).

This threshold is necessary for test reliability and reproducibility. If wind conditions are not bounded in some fashion in an outdoor fire test, large variances on product performance could be introduced due to varying wind conditions.

Mitigations

The investigation of the VBB fire identified several gaps in Tesla's commissioning procedures, electrical fault protection devices and thermal roof design. Since the fire, Tesla has implemented a number of procedural, firmware, and hardware mitigations to address these gaps. These mitigations have been applied to all existing and any future Megapack installations and include:

Procedural Mitigations:

- Improved inspection of the coolant system for leaks during Megapack assembly and during end-of-line testing to reduce the likelihood of future coolant leaks.
- Reduce the telemetry setup connection time for new Megapacks from 24 hours to 1 hour to ensure new equipment is transmitting telemetry data (internal temperatures, fault alarms, etc.) to Tesla's offsite control facility for remote monitoring.
- Avoid utilizing the Megapack's keylock switch during commissioning or operation unless the unit is
 actively being serviced. This procedural mitigation ensures telemetry, fault monitoring, and electrical
 fault safety devices (such as the pyro disconnect) are active while the Megapack is idle (such as during
 testing and commissioning).

Firmware Mitigations:

- Added additional alarms to the coolant system's telemetry data to identify and respond (either manually or automatically) to a possible coolant leak.
- Keep all electrical safety protection devices active, regardless of keylock switch position or system state. This firmware mitigation allows electrical safety protection devices (such as the pyro disconnect) to remain in an active mode, capable of actuating when electrical faults occur at the battery modules, no matter what the system status is.
- Active monitoring and control of the pyro disconnect's power supply circuit. In the event of a power supply failure (either through an external event such as a coolant exposure or some other means), the Megapack will automatically actuate the pyro disconnect prior to the loss of its power supply.

Hardware Mitigations

• Installation of newly designed, thermally insulated steel vent shields within the thermal roof of all Megapacks. These vent shields protect the plastic overpressure vents from direct flame impingement or hot gas intrusion, thus keeping the IP66 battery bay enclosures isolated from a fire above in the thermal roof. Their performance was validated through a series of fire tests, including unit level fire testing of entire Megapack units.¹³ The vent shields are placed over the top of the overpressure vents and will come standard on all new Megapack installations. For existing Megapacks, the vent shields can be installed in the field (retrofit) with minimal effort or disruption to the unit. At the time of this report, the vent shields are nearing production stage and will be retrofitted to applicable Megapack sites shortly.

The tests confirmed that, even with the entire thermal roof fully involved in fire, the overpressure vents will not ignite and the battery modules below remain relatively unaffected by the fire above. For instance, the cells within the battery modules saw a less than 1°C temperature rise while the entire thermal roof was fully involved in fire.

Emergency Response

Beyond the origin and cause and propagation investigations, another key aspect of the VBB fire was the emergency response. The CFA is the responsible fire service organization for VBB, and the facility is in their initial response jurisdiction. The location of the VBB facility is in a semi-rural location. The nearest fire station is the CFA Lovely Banks, approximately 4 km (2.5 miles) distance from VBB and thus relatively close, though other resources had more extended travel distances.

Upon arrival around 10:30 AM, CFA immediately established incident command (IC) in accordance with their protocols, and the IC worked closely with the facility representatives and subject matter experts (SMEs). This close coordination continued throughout the entire event. The facility was evacuated and all-site personnel accounted-for upon notification of the emergency event and the commencement of fire service operations. A 25 m (82 ft) perimeter was established around MP-1 while water application and cooling strategies were discussed with facility representatives and subject matter experts (SMEs). The decision was made to provide exposure protection to Megapacks and transformers adjacent to MP-1 and MP-2 using water hose lines, as recommended in Tesla's ERG. The fire eventually propagated into MP-2; however, flame spread did not advance any further than MP-1 and MP-2. The two Megapacks were permitted to burn themselves out, during which time the CFA did not directly apply water into or onto either Megapack. By 4:00 PM (approximately six hours after the start of the event), visible flames had subdued and a fire watch was instituted. The CFA continued to monitor the site for the next three days before deeming it under control on August 2, 2021, at which time, the fire investigation began.

Key Takeaways

A thorough review of the VBB fire emergency response yielded the following key takeaways:

- Effective Pre-incident Planning: VBB had both an Emergency Action Plan (EAP) and an Emergency Response Plan (ERP). Both plans were available to emergency responders and were effectively used during the VBB fire. For example, all site employees and contractors followed proper evacuation protocols during the fire and as a result, no injuries occurred to those personnel.
- Coordination with SMEs: VBB had thorough pre-incident plans that clearly identified the SMEs, how to
 contact them, their role and other key tasks. It was reported that the facility SMEs stayed in close
 contact with the CFA IC throughout the VBB fire, providing valuable information and expertise for the
 CFA to draw upon. For example, site representatives and SMEs worked closely with the CFA in
 determining water application and cooling strategies of adjacent exposures.
- Water Application: A key question regarding water application is the necessary amount and duration for effective fire containment. Tesla's design philosophy is based on inherent passive protection (i.e., thermal insulation), with minimal dependence on active firefighting measures like external hose lines. As such, water was not aimed at suppressing the fire but rather protecting the exposures as directed by Tesla's ERG and the SMEs on site. All available data and visual observations of the fire indicates water had limited effectiveness in terms of reducing or stopping fire propagation from Megapack-to-Megapack. The thermal insulation appears to be the dominant factor in reducing heat transfer between adjacent Megapacks. However, water was effectively used on other exposures

- (transformers, electrical equipment, etc.) to protect that equipment, which are not designed with the same level of protection as a Megapack is (i.e., thermal insulation).¹⁴
- The fire protection design approach of the Megapack has inherent advantages over other BESS designs in terms of safety to emergency responders. The Megapack approach minimizes the likelihood of fire spread using passive compartmentation and separation, eliminates the danger to fire fighters of an overpressure event due to design features and a lack of confinement (e.g., outdoor versus indoor), does not rely on active firefighting measures like external hose lines and minimizes the dangers from stranded electrical energy to those involved with overhaul and de-commissioning with a fire response approach permitting the Megapack to burn itself out.

Environmental Concerns

The Environment Protection Authority Victoria (EPA) deployed two mobile air quality monitors within 2 km (1.2 miles) of the VBB site. Locations were chosen where there was potential to impact the local community. The EPA monitors confirmed "good air quality in the local community" after the incident; however, the measurements were not taken during the peak of the fire event. They were sampled around 6:00 PM, or approximately 2 hours after the fire was out. Therefore, the data cannot be used to understand the airborne hazards during the actual fire event. The data does demonstrate that two hours after the fire event, the air quality in the surrounding area was "good" and no long-lasting air quality concerns arose from the fire event.¹⁵

During the fire event, the CFA coordinated with site personnel to control the water run-off from fire hoses into a catchment. Water samples, collected by Tesla site personnel under the supervision of CFA, were extracted from the catchment. Laboratory results from those samples indicated that the likelihood of the fire having a material impact on the water was minimal. After the incident, as a precaution, the water was removed from the catchment, via suction trucks, and was transported to a licensed waste facility for treatment and disposal. It is estimated that approximately 900,000 liters of water was disposed of from the site after the event.

Community Concerns

Neoen, the project developer and owner, pro-actively engaged with the local community during and following the VBB fire. These engagements included door-to-door visits, phone calls and emails with the residential and agricultural properties within a 2-3 km (1.2-1.9 mile) radius of the VBB site. Neoen found their prior community outreach during the project planning stages to be invaluable as this outreach provided up-to-date contact information for Neoen when reaching out to the local community during and following the fire. In addition, Neoen formed an executive stakeholder steering committee compromising of key organizations within 24 hours of the incident. With multiple parties involved in the emergency response to the fire event

At the time of this report, final fire department reports were not available for review and inclusion. As that information becomes available, additional information regarding water usage and effectiveness may require inclusion in this report. Although the effectiveness of external water in a Megapack fire may be limited, water should still be made available for exposure protection and other unanticipated events in the future, as required by any applicable regulatory requirements.

It should be noted that prior regulatory testing (UL 9540A module level fire testing) has shown that the products of combustion of a Megapack battery module can include flammable and nonflammable gases. Based on those regulatory tests, the flammable gases were found to be below their lower flammable limit (LFL) and would not pose a deflagration or explosion risk to first responders or the general public. The nonflammable gases were found to be comparable to the smoke you would encounter in a typical Class A structure fire and do not contain any unique, or atypical, gases beyond what you would find in the combustion of modern combustible materials.

actively participating in the steering committee, this helped ensure that from the outset communication was timely, efficient, well-coordinated across different organizations and accurate.

In addition to the community outreach, Neoen and Tesla also briefed multiple industry, State and Federal Government Departments and Agencies immediately following the VBB fire and at the conclusion of the investigation process. These briefings helped ensure the wider energy sector with interests in BESS were able to be kept directly informed as information became available.

Overhaul and Remediation

On July 29, 2021 nearly half of the Megapacks had been installed and the site was in the testing and commissioning stage of the project. Following the fire event on July 30, 2021, fire department personnel, regulatory agencies and other emergency responders remained on-site for precautionary purposes until August 2, 2021. At that time the site was turned over for regulatory fire investigations to begin. On-site fire investigations started on August 3, 2021 and continued until August 12, 2021. During this time, starting on August 6, 2021, the site was permitted to continue the installation of Megapacks while the area around MP-1 remained cordoned off for the investigation. On September 23rd, 2021, less than two months after the fire, VBB was re-energized and testing and commissioning restarted. Remediation of the damaged equipment followed shortly after, and lasted a total of three days. All testing and commissioning efforts were completed without any further incidents and on December 8, 2021, VBB officially opened.

Lessons Learned

The VBB fire exposed a number of unlikely factors that, when combined, contributed to the fire initiation as well as its propagation to a neighboring unit. This collection of factors had never before been encountered during previous Megapack installations, operation and/or regulatory product testing. This section summarizes those factors as well as the emergency response to the fire, discusses the lessons learned from this fire event, and highlights the mitigations Tesla has implemented in response.

1. Commissioning Procedures

Lessons learned related to commissioning procedures include: (1) limited supervision/monitoring of telemetry data during the first 24 hours of commissioning and (2) the use of the keylock switch during commissioning and testing. These two factors prevented MP-1 from transmitting telemetry data (internal temperatures, fault alarms, etc.) to Tesla's control facility and placed critical electrical fault safety devices (such as the pyro disconnect) in a state of limited functionality, reducing the Megapack's ability to actively monitor and interrupt electrical fault conditions prior to them escalating into a fire event.

Since the VBB fire, Tesla has modified their commissioning procedures to reduce the telemetry setup connection time for new Megapacks from 24 hours to 1 hour and to avoid utilizing the Megapack's keylock switch unless the unit is actively being serviced.

2. Electrical Fault Protection Devices

Lessons learned related to electrical fault protection devices include: (1) coolant leak alarms; (2) the pyro disconnect being unable to interrupt fault currents when the Megapack is off via the keylock switch and (3) the pyro disconnect likely being disabled due to a power supply loss to the circuit that actuates it. These three factors prevented the pyro disconnect of MP-1 from actively monitoring and interrupting the electrical fault conditions before escalating into a fire event.

Since the VBB fire, Tesla has implemented a number of firmware mitigations that keep all electrical safety protection devices active, regardless of keylock switch position or system state, and to actively monitor and control the pyro disconnect's power supply circuit. Furthermore, Tesla has added additional alarms to better identify and respond (either manually or automatically) to coolant leaks. Additionally, although this fire event was likely initiated by a coolant leak, unexpected failures of other internal components of the Megapack could create similar damage to the battery modules. These new firmware mitigations do not only address damage from a coolant leak. They also permit the Megapack to better identify, respond, contain and isolate issues within the battery modules due to failures of other internal components, should they occur in the future.

3. Fire Propagation

Lessons learned related to fire propagation include: (1) the significant role external, environmental conditions (such as wind) can have on a Megapack fire and (2) the identification of a weakness in the thermal roof design that permits Megapack-to-Megapack fire propagation. These two factors led to direct flame impingement on the plastic overpressure vents that seal the battery bay from the thermal roof. With a direct path for flames and hot gases to enter into the battery bays, the cells within the battery modules of MP-2 failed and became involved in the fire.

Since the VBB fire, Tesla has devised (and validated through extensive testing) a hardware mitigation that protects the overpressure vents from direct flame impingement or hot gas intrusion via the installation of new, thermally insulated, steel vent shields. The vent shields are placed on top of the overpressure vents and will come standard on all new Megapack installations. For existing Megapacks, the vent shields can be easily installed in the field. At the time of this report, the vent shields are nearing production stage and will be retrofitted to applicable Megapack sites shortly.

4. Megapack Spacing

Lessons learned related to Megapack spacing include: no changes are required to the installation practices of the Megapack with the vent shield mitigation (as described above) in place. Based on an analysis of telemetry data within MP-2 during the VBB fire, the Megapack's thermal insulation can provide significant thermal protection in the event of a fire within an adjacent Megapack installed 15 cm (6 in) away. The internal cell temperatures of MP-2 only increased by 1°C (1.8°F), from 40°C to 41°C (104°F to 105.8°F), before communication was lost to the unit, presumably due to fire, around 11:57 AM (approximately 2 hours into the fire event). Fire propagation was triggered by the weakness in the thermal roof, as described above in #3, and not due to heat transfer via the 15 cm (6 in) gap between Megapacks. With the vent shield mitigation in place, the weakness has been addressed and validated through unit level fire testing (i.e., tests involving the ignition of the Megapack's thermal roof). These tests confirmed that, even with the thermal roof fully involved in a fire, the overpressure vents will not ignite and the battery modules remain relatively unaffected with internal cell temperatures rising less than 1°C.

5. Emergency Response

Lessons learned from the emergency response to the VBB fire include: (1) effective pre-incident planning is invaluable and can reduce the likelihood of injuries; (2) coordination with SMEs, either on site or remotely, can provide critical expertise and system information for emergency responders to draw upon; (3) the effectiveness of applying water directly to adjacent Megapacks appears to provide limited benefits; however, water application to other electrical equipment, with inherently less fire protection built into their designs (such as transformers), can be a useful tactic to protect that equipment; (4) the fire protection design

approach of the Megapack has inherent advantages over other BESS designs in terms of safety to emergency responders; (5) the EPA indicated that there was "good" air quality 2 hours after the fire demonstrating that no long-lasting air quality concerns arose from the fire event; (6) water samples indicated that the likelihood of the fire having a material impact on firefighting water was minimal; (7) prior community engagement during the project planning stages is invaluable as it enabled Neoen to quickly update the local community and address immediate questions and concerns; (8) early, factual and where possible, face-to-face engagement with the local community is essential when a fire event is unfolding to keep the general public informed; (9) an executive stakeholder steering committee from the key organizations involved in the emergency response can help ensure that any pubic communications are timely, efficient, coordinated and accurate; and (10) effective coordination between stakeholders at the site allowed for rapid and thorough handover process after the incident, the swift and safe decommissioning of the damaged units and the site's quick return to service.

In summary, the VBB fire event proceeded in accordance with its fire protection design and pre-incident planning. It presented no unusual, unexpected, or surprising characteristics (i.e., explosions) or resulted in any injuries to site personnel, the general public or emergency responders. It was isolated to the units directly involved, had minimal environmental impact, did not adversely impact the electrical grid, and had appreciably short mission interruption.

ATTACHMENT 6 SCIENTIFIC REPORT FROM NATURE ON HF EMISSIONS FROM LITHIUM ION BATTERIES.

OPEN Toxic fluoride gas emissions from lithium-ion battery fires

Fredrik Larsson^{1,2}, Petra Andersson², Per Blomqvist² & Bengt-Erik Mellander¹

Lithium-ion battery fires generate intense heat and considerable amounts of gas and smoke. Although the emission of toxic gases can be a larger threat than the heat, the knowledge of such emissions is limited. This paper presents quantitative measurements of heat release and fluoride gas emissions during battery fires for seven different types of commercial lithium-ion batteries. The results have been validated using two independent measurement techniques and show that large amounts of hydrogen fluoride (HF) may be generated, ranging between 20 and 200 mg/Wh of nominal battery energy capacity. In addition, 15-22 mg/Wh of another potentially toxic gas, phosphoryl fluoride (POF₃), was measured in some of the fire tests. Gas emissions when using water mist as extinguishing agent were also investigated. Fluoride gas emission can pose a serious toxic threat and the results are crucial findings for risk assessment and management, especially for large Li-ion battery packs.

Lithium-ion batteries are a technical and a commercial success enabling a number of applications from cellular phones to electric vehicles and large scale electrical energy storage plants. The occasional occurrences of battery fires have, however, caused some concern especially regarding the risk for spontaneous fires and the intense heat generated by such fires¹⁻⁵. While the fire itself and the heat it generates may be a serious threat in many situations, the risks associated with gas and smoke emissions from malfunctioning lithium-ion batteries may in some circumstances be a larger threat, especially in confined environments where people are present, such as in an aircraft, a submarine, a mine shaft, a spacecraft or in a home equipped with a battery energy storage system. The gas emissions has however only been studied to a very limited extent.

An irreversible thermal event in a lithium-ion battery can be initiated in several ways, by spontaneous internal or external short-circuit, overcharging, external heating or fire, mechanical abuse etc. This may result in a thermal runaway caused by the exothermal reactions in the battery⁶⁻¹⁰, eventually resulting in a fire and/or explosion. The consequences of such an event in a large Li-ion battery pack can be severe due to the risk for failure propagation¹¹⁻¹³. The electrolyte in a lithium-ion battery is flammable and generally contains lithium hexafluorophosphate (LiPF₆) or other Li-salts containing fluorine. In the event of overheating the electrolyte will evaporate and eventually be vented out from the battery cells. The gases may or may not be ignited immediately. In case the emitted gas is not immediately ignited the risk for a gas explosion at a later stage may be imminent. Li-ion batteries release a various number of toxic substances 14-16 as well as e.g. CO (an asphyxiant gas) and CO₂ (induces anoxia) during heating and fire. At elevated temperature the fluorine content of the electrolyte and, to some extent, other parts of the battery such as the polyvinylidene fluoride (PVdF) binder in the electrodes, may form gases such as hydrogen fluoride HF, phosphorus pentafluoride (PF₅) and phosphoryl fluoride (POF₃). Compounds containing fluorine can also be present as e.g. flame retardants in electrolyte and/or separator¹⁷, in additives and in the electrode materials, e.g. fluorophosphates 18,19, adding additional sources of fluorine.

The decomposition of LiPF₆ is promoted by the presence of water/humidity according to the following reactions^{20,21};

$$LiPF_6 \rightarrow LiF + PF_5 \tag{1}$$

$$PF_5 + H_2O \rightarrow POF_3 + 2HF \tag{2}$$

$$LiPF_6 + H_2O \rightarrow LiF + POF_3 + 2HF$$
 (3)

¹Department of Physics, Chalmers University of Technology, Kemivagen 9, SE-41296, Gothenburg, Sweden. ²Safety and Transport, RISE Research Institutes of Sweden, Brinellgatan 4, SE-50115, Boras, Sweden. Correspondence and requests for materials should be addressed to F.L. (email: vegan@chalmers.se)

Received: 11 April 2017 Accepted: 28 July 2017

Published online: 30 August 2017

Battery	Numbers of batteries per test	Туре	Nominal capacity per battery (Ah)	Nominal voltage per battery (V)	Cell packaging
A	5–10	LCO (LiCoO ₂)	6.8	3.75	Prismatic hard Al-can
В	2	LFP (LiFePO ₄)	20	3.2	Pouch
С	5	LFP (LiFePO ₄)	7	3.2	Pouch
D	9	LFP (LiFePO ₄)	3.2	3.2	Cylindrical
E	5	LFP (LiFePO ₄)	8	3.3	Cylindrical
F	2	NCA-LATP (LiNiCoAlO ₂ -LiAlTiPO ₄)	30	2.3	Pouch
G	2	Laptop pack*	5.6	11.1	Cylindrical

Table 1. Details of the tested Li-ion battery cells. *Each laptop battery pack has 6 cells of type 18650; arranged 2 in parallel and 3 in series.

Of these PF₅ is rather short lived. The toxicity of HF and the derivate hydrofluoric acid is well known^{22–24} while there is no toxicity data available for POF₃, which is a reactive intermediate²⁵ that will either react with other organic materials or with water finally generating HF. Judging from its chlorine analogy POCl₃/HCl²⁴, POF₃ may even be more toxic than HF. The decomposition of fluorine containing compounds is complex and many other toxic fluoride gases might also be emitted in these situations, however, this study focuses on analysis of HF and POF₃.

Although a number of qualitative and semi-quantitative attempts have been made in order to measure HF from Li-ion batteries under abuse conditions, most studies do not report time dependent rates or total amounts of HF and other fluorine containing gases for different battery types, battery chemistries and state-of-charge (SOC). In some measurements reported, HF has been found, within limited SOC-variations, during the abuse of Li-ion battery cells^{15,16,26}, as well as detected during the abuse of battery packs²⁷. However, time-resolved quantitative HF gas emission measurements from complete Li-ion battery cells undergoing an abusive situation have until now only been studied to a limited extend; for a few SOC-values, including larger commercial cells^{28,29}, a smaller-size commercial cells³⁰ and a research cell (i.e. non-commercial cell)³¹. Time-resolved quantitative HF measurements on the gas release from complete electric vehicles including their Li-ion battery packs during an external fire have also been performed³². Other types of gas emissions from Li-ion cells during abuse have been the subject of a somewhat larger number of investigations³³⁻⁴¹. Since the electrolyte typically is the primary source of fluorine, measurements of fluorine emissions from battery type electrolytes have been studied. For example, fire or external heating abuse tests have been performed on electrolytes⁴²⁻⁴⁶ and the quantitative amounts of HF and POF₃ have been measured in some cases^{45,46}. Other studies of electrolytes exposed to moderate temperatures, 50–85 °C, show the generation of various fluorine compounds^{20,21,47-49} and some studies include both electrolyte and electrode material^{50,51,52}.

Our quantitative study of the emission gases from Li-ion battery fires covers a wide range of battery types. We found that commercial lithium-ion batteries can emit considerable amounts of HF during a fire and that the emission rates vary for different types of batteries and SOC levels. POF₃, on the other hand, was found only in one of the cell types and only at 0% SOC. The use of water mist as an extinguishing agent may promote the formation of unwanted gases as in eqs (2)–(3) and our limited measurements show an increase of HF production rate during the application of water mist, however, no significant difference in the total amount of HF formed with or without the use of water mist.

Lithium-ion battery fire tests. The experiments were performed using an external propane burner for the purpose of heating and igniting the battery cells as described in the Methods section. Seven different types of batteries, type A-G, were investigated, from seven manufacturers and with different capacity, packaging type, design and cell chemistry, as specified in Table 1. Type A had a lithium cobalt oxide (LCO) cathode and carbon anode, types B to E had lithium-iron phosphate (LFP) cathode and carbon anode, type F had nickel cobalt aluminum oxide (NCA) and lithium aluminum titanium phosphate (LATP) electrodes while type G was a laptop battery pack with unspecified battery chemistry. All electrolytes contained LiPF₆. Most of the cells were tested for different SOC levels, from fully charged, 100% SOC, to fully discharged, 0% SOC. The study included large-sized automotive-classed cells, i.e. series production cells of high industry quality, with long life time etc.

The heat release rate (HRR) and the emitted HF for B-type cells with different SOC values are shown in Fig. 1. Only the 100% SOC cells show several distinct peaks, corresponding to intense flares, when the cells vented and the emitted gas burn, for all other cells the heat release as a function of time is more smooth. These behaviors are reproducible also for the other tested cell types, e.g., only the 100% SOC cells show the more violent heat release peaks with intense flares.

The measurements of the gas emissions during the fire tests show that the production of HF is correlated to the increase in HRR although somewhat delayed. From Fig. 1b it is evident that the higher SOC value, the higher values for the peak HF release rate. The total amount of HF varies considerably for the different battery types, see Fig. 2a. The amount of HF produced, expressed in mg/Wh, where Wh is the nominal battery energy capacity, is approximately 10 times higher for the cell with the highest values compared to the cells with the lowest values. The different relative amount of electrolyte and filler materials in the cells could be the simple explanation of this variation but information on those amounts are difficult to access for commercial batteries. The highest HF values are found for the pouch cells, a possible explanation would be that hard prismatic and cylindrical cells can build a

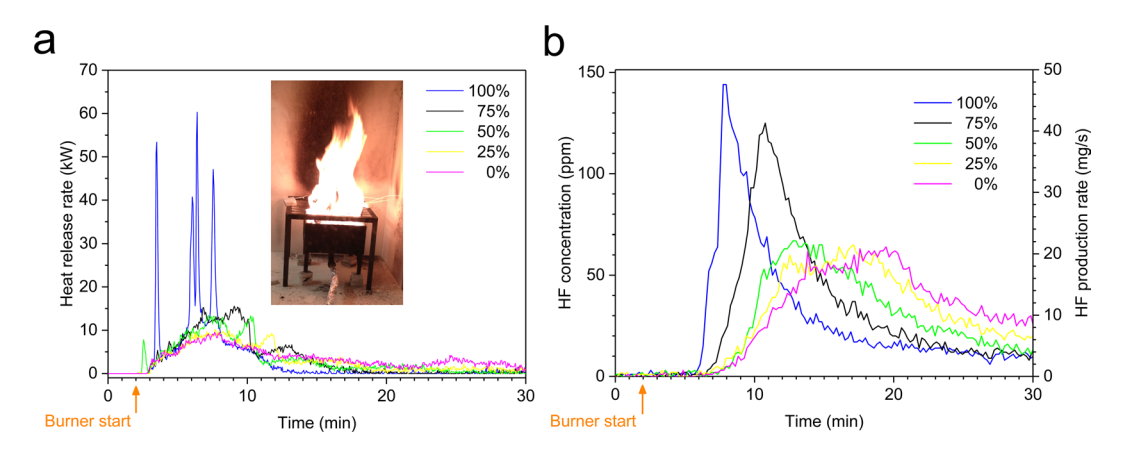


Figure 1. Results for type B cells, for 0–100% SOC with intermediate SOC-steps of 25%, exposed to an external propane fire; (**a**) showing the heat release rate (burner HRR contribution is subtracted), the inset photo shows burning battery cells during the test; (**b**) showing the HF release both as the measured concentrations as well as the calculated HF production rates. The HF production rates are calculated from the measured HF concentration by the Ideal gas law taking into account the ventilation flow, see Methods. The starting time of the heating process is marked on the time axis.

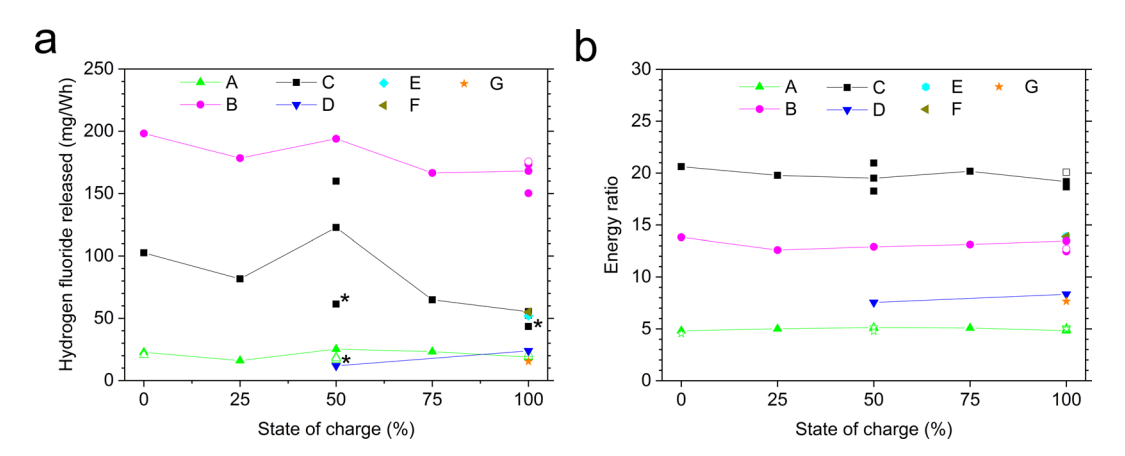


Figure 2. Total amount of HF measured by FTIR, normalized to nominal electrical energy capacity (**a**) and the energy ratio (**b**), for seven types of Li-ion battery cells and with various state of charge levels. Non-filled symbols indicate a repetition variant, e.g. applying water mist. The lines are intended as a guide for the eye. The energy ratio is a dimensionless value calculated by taking the total heat release from the battery fire divided by the nominal electrical energy capacity. Note that for 100% SOC the values are overlapping for type C, E and F as well as for type A, D and G in (**a**) and type B, E and F in (**b**). *Low value for type C at 50% and 100% SOC and type D at 50% SOC due to that a pre HF-saturation was not applied, therefore a part of the HF release was likely to be saturated in the gas sampling system, see Methods.

higher pressure before bursting, rapidly releasing a high amount of gases/vapors from the electrolyte. Due to the high velocity of the release and thus the short reaction time, combustion reactions might be incomplete and less reaction products might be produced. In the test involving type G the cylindrical cells were layered horizontally, thus having a different venting direction and possibly increased wall losses, which combined with a very energetic response, might suggest why HF was detected only from the filter analysis and not detected by FTIR-analysis. The tested pouch cells of type B and C burned for longer time and with less intensity. The pouch cell of type F, however, burned faster, possibly due to its different electrode materials. The SOC influence on the HF release was less significant and the trend in Fig. 2a shows higher HF values for 0% than for 100% SOC, however with clear peaks at 50% SOC. Although these results are reproducible, they are difficult to explain. In other studies^{30,31}, significantly narrower in test scope, involving smaller-sized cells and using a somewhat different abuse method, it was found that the total amount of HF measured by real-time FTIR was higher for decreasing SOC (tests conducted at 100%, 50% and 0% SOC).

The HRR curve is used to calculate the total heat release (THR) which corresponds to the energy released from the burning battery. THR is obtained by integrating the measured HRR (with the burner contribution subtracted) over the complete test time. Fig. 2b shows the energy ratio, that is how much energy is produced by the burning

Battery	Nominal energy capacity (Wh)	Normalized total HF detected with FTIR (mg/Wh)	Normalized maximum HRR (W/Wh)	Normalized THR (kJ/Wh)
A	128	15-25	243-729	17–19
В	128	150-198	78-633	45-50
С	112	43-160	116-491	66-75
D	92	12-24	207-315	27-30
E	132	52	235	50
F	138	55	384	50
G	124	15	460	28

Table 2. Main test results normalized to nominal energy capacity, when applicable including various SOC-levels

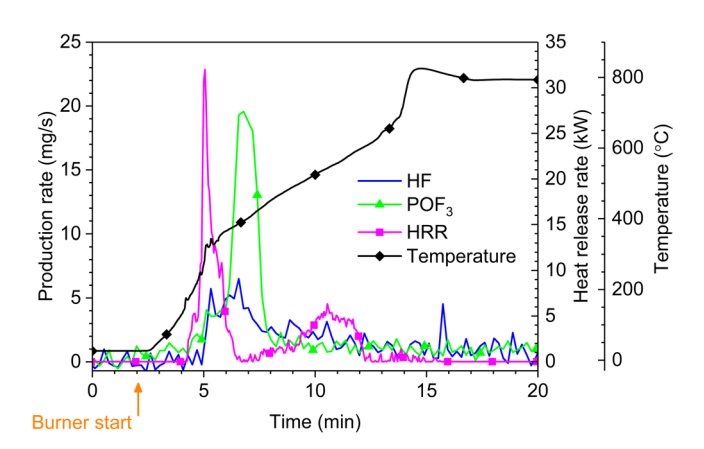


Figure 3. Results for a test with 5 type A cells at 0% SOC showing HF and POF₃, HRR and average surface temperature of the battery cells.

battery, compared to the amount of nominal electrical energy capacity a fully charged battery can deliver to an external circuit. The energy ratio is therefore a comparison between the chemical and the electrical energy of the Li-ion battery cell. The energy ratio varies considerably for the different cell types but is approximately constant for each cell, independent of SOC level. There are some similarities in Fig. 2a and b for the pouch cells, type B and C, which give the highest values in both cases, although in reverse order. This might indicate a higher amount of combustibles, e.g. electrolyte, in these cells compared to the other cells. It is also interesting to see that the energy ratio varies significantly between the tested cells, ranging from 5 to 21. This is important knowledge for fire protection and fire fighting. The energy ratio thus refers to a nominal fully charged battery while in normal use only a part of the SOC-window is used, for example half (50%) of the SOC-window (corresponding to cycling the battery between e.g. 30% and 80% SOC). If instead, the total heat release divided by the used electric battery capacity in the specific application is considered, higher energy ratio values are obtained. A summary of the results is shown in Table 2.

The measured heat release from an overheated battery may include several aspects, e.g. the battery temperature increase and the combustion of released gases. Variations due to the type of battery cell, the initiation method, e.g. if the test is done as an external fire test, an external heating or an overcharge test, and the test method, e.g. access to ambient oxygen (inert, under-ventilated or well-ventilated fire), and the presence of an external igniter, can greatly affect the amount of measured heat release. Energy release from a internal cell event in a confined environment can, for example, be lower than the energy release from the same cell in case of external fire. Thus energy ratios published using other methods and other types of Li-ion cells can be significantly different^{7,52,53}.

For all tested battert types and selected SOC-levels, POF₃ could only be measured quantitatively for type A battery cells at 0% SOC. Repeated measurements confirmed the presence of POF₃ only for type A and only for 0% SOC. No POF₃ could thus be detected in any of the other tests. POF₃ is an intermediate compound and the local combustion conditions in every test, will influence the amounts of POF₃ generated. This shows the importance of investigating many different set-ups when evaluating emitted gases.

In Fig. 3 the HRR, the average surface temperature of the five cells as well as the HF and POF₃ production rates are shown for type A cells at 0% SOC. The POF₃ curve is less noisy than the HF curve due to different signal-to-noise ratios of the FTIR instrumentation at the different wavenumbers. There is a secondary peak in HRR approximately 5 minutes after the main heat event, this peak does not correspond to any peaks in the mass flow of HF or POF₃. The explanation for this could be that the second peak in the heat release rate involves burning of mainly non-fluorine containing compounds. The temperature curve shows a rapid increase above the

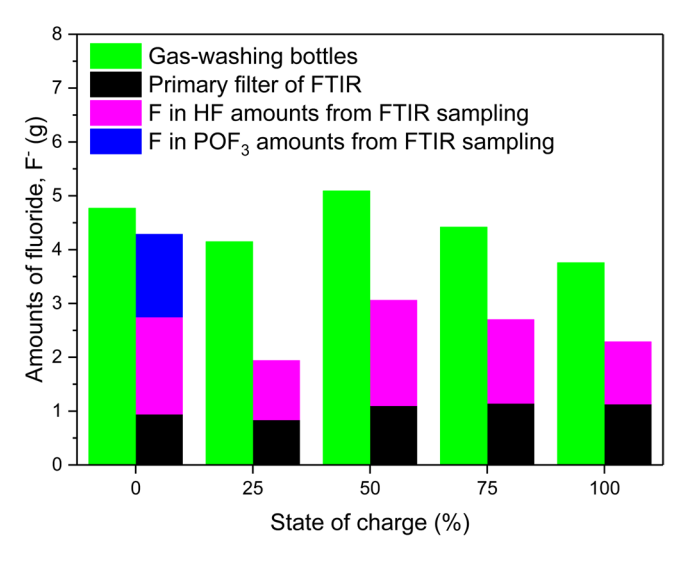


Figure 4. Total amount of measured fluoride, F, for type A, for 0–100% SOC with intermediate steps of 25%. The amount of F from the FTIR is calculated from the measurement results for POF₃ and HF, while the amount of fluoride from gas-washing bottles and primary filter analyses is measured as water soluble fluoride.

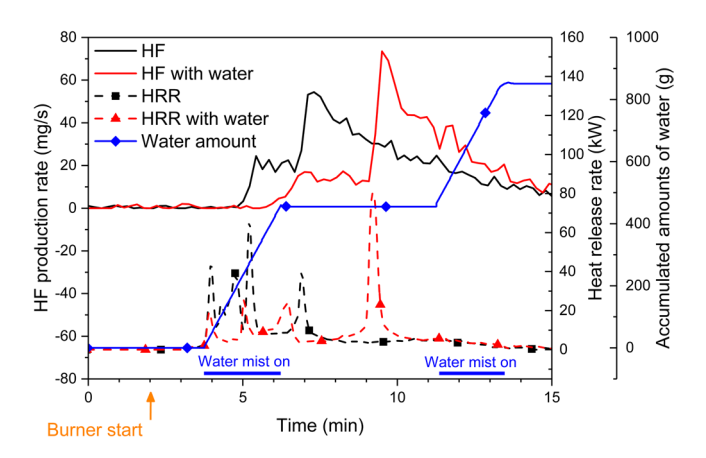


Figure 5. Results for type B cells at 100% SOC with and without the use of water mist.

melting temperature of the alumina cell case at about $660\,^{\circ}$ C. At these temperatures the alumina is molten and has formed a puddle on the burner bed beneath the battery cells. The thermal conditions in and around the thermocouples and the remains of the batteries have therefore changed considerably causing the apparent temperature increase.

In addition to the time resolved measurements with the FTIR, gas-washing bottles were used to determine the total fluorine content in the gas emissions during the tests. A comparison between the different measurement methods used can be seen in Fig. 4 for type A cells. Note that the FTIR measurements are performed only to detect HF and POF₃, other fluoride compounds are not included. It is interesting to note that for 0% SOC the total amount of fluoride measured by the gas-washing bottle technique matches rather well with the FTIR and primary filter analysis. For other SOC values the fluoride content is higher from the gas-washing bottle measurements. Still, the general trend observed in the FTIR measurements for different SOC values is more or less confirmed by the gas-washing bottle measurements.

Gas-washing bottles were also used for some of the tests involving battery types B and C. These batteries showed higher amounts of released HF compared to type A. The ratio between the total values of released flouride from FTIR plus filter analysis and from the gas-washing bottles for type B and C was between 0.89 and 1.02, indicating a better correlation between FTIR and gas-washing bottles measurement when HF gas emissions are higher.

The total amount of POF₃ measured by FTIR for type A at 0% SOC was 2.8 g (for 5-cells) and 3.9 g (for 10 cells). Hence, the normalized total POF₃ production was 15–22 mg/Wh of nominal battery energy capacity. Abuse studies measuring POF₃ are few, Andersson *et al.*⁴⁶ found both HF and POF₃ when burning mixtures of propane and Li-ion battery electrolytes with a HF:POF₃ production ratio between 8:1 and 53:1. Besides HF and POF₃ measurements, several distinct non-assigned peaks were found in the FTIR measurements, e.g. at 1027 cm⁻¹

			Normalized total HF de	etected (mg/Wh)		
Battery	SOC (%)	Number of tests	From FTIR	From gas-washing bottles	Normalized maximum HRR (W/Wh)	Normalized THR (kJ/Wh)
	100	6	19.8 ± 1.2 [3]	29.1 ± 3.1 [5]	612 ± 102	18.1 ± 0.46
A	50	7	18.5 ± 3.9 [6]	36.7 ± 3.3 [6]	416±39 [6]	18.0±0.61 [6]
	0	2	21.6 ± 1.5	38.3 ± 1.6	214±53	16.8±0.66
В	100	4	166.8 ± 11.5	191.3 ± 11.3 [2]	538±77	46.9 ± 1.9
С	100	3	53.9 ± 2.0 [2]*	N/A	461 ± 27	69.5 ± 2.6
	50	3	141.3 ± 26.3 [2]*	N/A	149±5	70.5 ± 4.9

Table 3. Detailed results for all available repetitions. Values presented as mean values followed by the standard deviation, in case the data parameter was not measured in all tests the value in bracket declares the number of available tests used for the specific data parameter value. *For FTIR data for battery type C, one data point of 50% and one data point at 100% SOC are excluded as outliers since they were low due to that a pre HF-saturation was not applied in the test, see Methods.

and 1034 cm⁻¹, which have also been seen in other studies⁴⁶. They are compatible with the typical C-O stretching energies of low molecular weight alcohols in gas phase but also with in-plane stretching of aromatic compounds. This indicates the complexity and the limited knowledge in this area.

Water mist measurements. In order to study the effects of water on gas emissions, fire tests have also been performed where a water mist was applied during the fire. The reason for this experiment is that water is the preferred extinguishing agent for a lithium-ion battery fire. The intention in this study was however not to extinguish the fire completely. One potential problem regarding the use of water mist is that the addition of water may, in principle, increase the rate of formation of HF, see Eqs (2) and (3).

Figure 5 shows the results for type B cells with and without exposure to water mist, note that both the HRR and HF production are delayed when water mist is used. In this limited study, the peak of the HF production rate increased by 35% when using water, however no significant change in the total amounts of the HF release could be seen. A similar result has been reported in a previous study²⁸. The water mist was applied during two different periods of time, as marked in Fig. 5, adding a total of 851 g of water in the reaction zone, however, several other large sources of water were also present in the experiment, i.e. water production from the propane combustion and from humidity in the air. The water mist is cooling the fire and the top surface of the pouch cell was for some time partly covered with liquid water; this is the reason that the battery fire is delayed as seen in Fig. 5. The water mist might actually also clean the air by collecting fume particles and HF can be bound to water droplets, thus possibly lowering the amount of HF in the smoke duct and increasing the non-measured amount of very toxic hydrofluoric acid on the test area surfaces (e.g. walls, floor, smoke duct walls).

Repeatability

Repeated tests were performed for battery types A-C for selected SOC-levels. Some of the repetitions included a variant, e.g. including water mist; see Methods. In Fig. 2 all available test data are presented. Since the test repetitions are not clearly observable in Fig. 2 the results are also presented in Table 3 showing the mean values and standard deviations and the number of performed tests. While the ranges in Table 2 include data for all tested SOC-values, Table 3 shows test data for repeated measurements including repetition variants.

Figure 6 shows the repeatability results for four tests of battery type B for 100% SOC. The time evolution of HRR varies in the fire tests as seen in Fig. 6a. In fire tests there are always natural variations, however comparing the tests with 100% SOC, in Fig. 6a, with those with lower SOC-values presented in Fig. 1a, the repeatability of the 100% SOC tests is significant. The third repetition (black line) in Fig. 6a is delayed due to that it included an application of water mist, as discussed above. Although the appearance of the HRR plots of the four tests differs in Fig. 6a the THR (the integrated HRR) values are rather similar. Fig. 6b shows the HF release for the same four tests of type B at 100% SOC. Repetition 2 and 3 were performed in the third test period, without secondary FTIR filter, and therefore Repetition 2 occurs earlier while Repetition 3 is delayed due to the applied water mist, as discussed above. For the four tests of type B at 100% SOC the mean value of the total FTIR detected HF release is 166.8 mg/Wh with a standard deviation of 11.5 mg/Wh, as seen in Table 3. Comparing Fig. 1b and Fig. 6b, shows that for 100% SOC the HF release is faster and reaches a higher value. Repetition 1 in Fig. 6b shows lower HF release peak values, however, the total HF release value from the FTIR measurement of 168 mg/Wh is close to the average value (166.8 mg/Wh, as seen in Table 3).

Conclusions

This study covered a broad range of commercial Li-ion battery cells with different chemistry, cell design and size and included large-sized automotive-classed cells, undergoing fire tests. The method was successful in evaluating fluoride gas emissions for a large variety of battery types and for various test setups.

Significant amounts of HF, ranging between 20 and 200 mg/Wh of nominal battery energy capacity, were detected from the burning Li-ion batteries. The measured HF levels, verified using two independent measurement methods, indicate that HF can pose a serious toxic threat, especially for large Li-ion batteries and in confined environments. The amounts of HF released from burning Li-ion batteries are presented as mg/Wh. If extrapolated for large battery packs the amounts would be 2–20 kg for a 100 kWh battery system, e.g. an electric

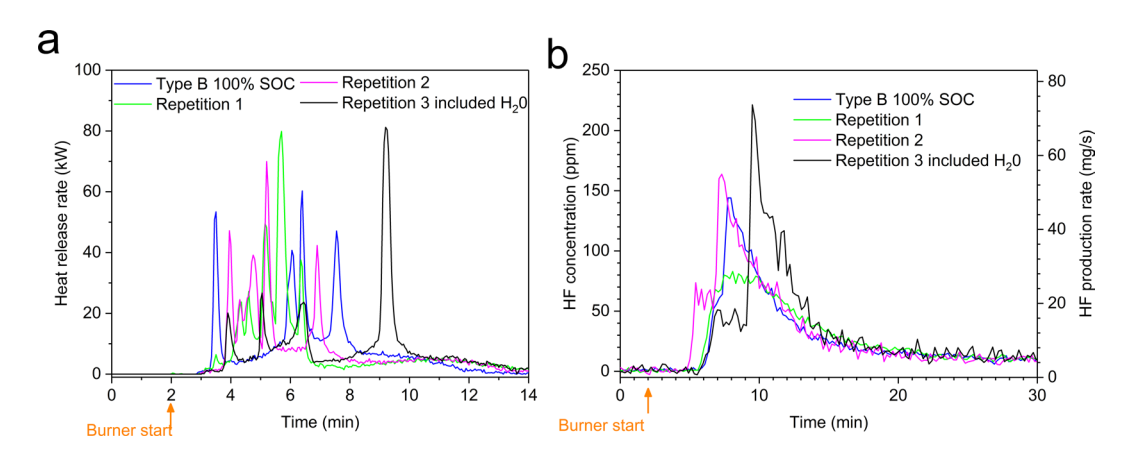


Figure 6. Repeatability for four tests of type B cells at 100% SOC, (**a**) shows the heat release rate (burner HRR contribution is subtracted) and (**b**) shows the HF release, both as the measured concentrations as well as the calculated HF production rates.

vehicle and 20–200 kg for a 1000 kWh battery system, e.g. a small stationary energy storage. The immediate dangerous to life or health (IDLH) level for HF is $0.025\,\text{g/m}^3$ (30 ppm)²² and the lethal 10 minutes HF toxicity value (AEGL-3) is $0.0139\,\text{g/m}^3$ (170 ppm)²³. The release of hydrogen fluoride from a Li-ion battery fire can therefore be a severe risk and an even greater risk in confined or semi-confined spaces.

This is the first paper to report measurements of POF₃, 15-22 mg/Wh, from commercial Li-ion battery cells undergoing abuse. However, we could only detect POF₃ for one of the battery types and only at 0% SOC, showing the complexity of the parameters influencing the gas emission. No POF₃ could be detected in any of the other tests.

Using water mist resulted in a temporarily increased production rate of HF but the application of water mist had no significant effect on the total amount of released HF.

The research area of Li-ion battery toxic gas emissions needs considerable more attention. Results as those presented here are crucial to be able to conduct a risk assessment that takes toxic HF gas into account. The results also enable strategies to be investigated for counteractions and safety handling, in order to achieve a high safety level for Li-ion battery applications. Today we have a rapid technology and market introduction of large Li-ion batteries but the risks associated with gas emissions have this far not been possible to take into consideration due to the lack of data.

Methods

Seven types of Li-ion batteries were exposed to an external propane fire. Fire characteristics, gas emissions, battery temperatures and cell voltages were measured. In total 39 fire tests were conducted of which 20 were within the base test matrix, 19 were repeated measurements of selected battery types and SOC-levels of which 10 included a variant, e.g. water mist for fire-fighting. The amounts of emitted fluoride gases were measured with two parallel and independent techniques, FTIR (time resolved concentration measurements and total values achieved by integration of the time resolved curve) and gas-washing bottles (total values). The experimental setup is schematically shown in Fig. 7. The gas collecting system and measurement system of the *Single Burning Item (SBI) method* (EN 13823⁵⁴), which is normally used for reaction-to-fire classification of construction products according to EN 13501-1⁵⁵ was used in the tests. The tests were performed in three different test periods; the second test period was conducted about 1 year after the first and the third test period was conducted about 2.5 years after the first. Each test period involved several days of testing. The measurement equipment, as specified in the text below, was somewhat varying between the three test periods.

Batteries. Six different types of Li-ion battery cells, type A-F, and one Li-ion battery pack, type G, were tested as seen in Table 1. The number of cells used in each test was varied in order to achieve similar electrical energy capacity per test. The batteries were placed on wire gratings just above a $16\,\mathrm{kW}$ propane burner. The wire grating was made of steel wire about 2 mm thick over a surface of about 300×300 mm. The quadrants of the grating were 40×100 mm. The cells were not electrically connected to each other (except the laptop packs of type G, see note in Table 1). Type A-F was pure battery cells while type G was a complete laptop battery pack which included plastics box, electronics and cables. The chemical content of the polymer materials in the auxiliary components of the battery pack of battery type G is not known. It is possible, however not likely, that fluorine was included in some of the components, which in that case could have resulted in the production of HF. For battery type A, 5 cells/test was used except in two variant tests in which 10 cells/test were used.

The influence of different state of charge was investigated, for some battery types the complete SOC-window ranging from 0% to 100%, with intermediate steps of 25%, was investigated. The SOC levels included for each battery type and the numbers of repetitions per test type, i.e. the fire test matrix, is seen in Table 4. All parameters were not measured in all of the tests. Measurement of HRR and corresponding THR was conducted in 38 tests, FTIR in 35 tests and gas-washing bottles were used in 19 tests.

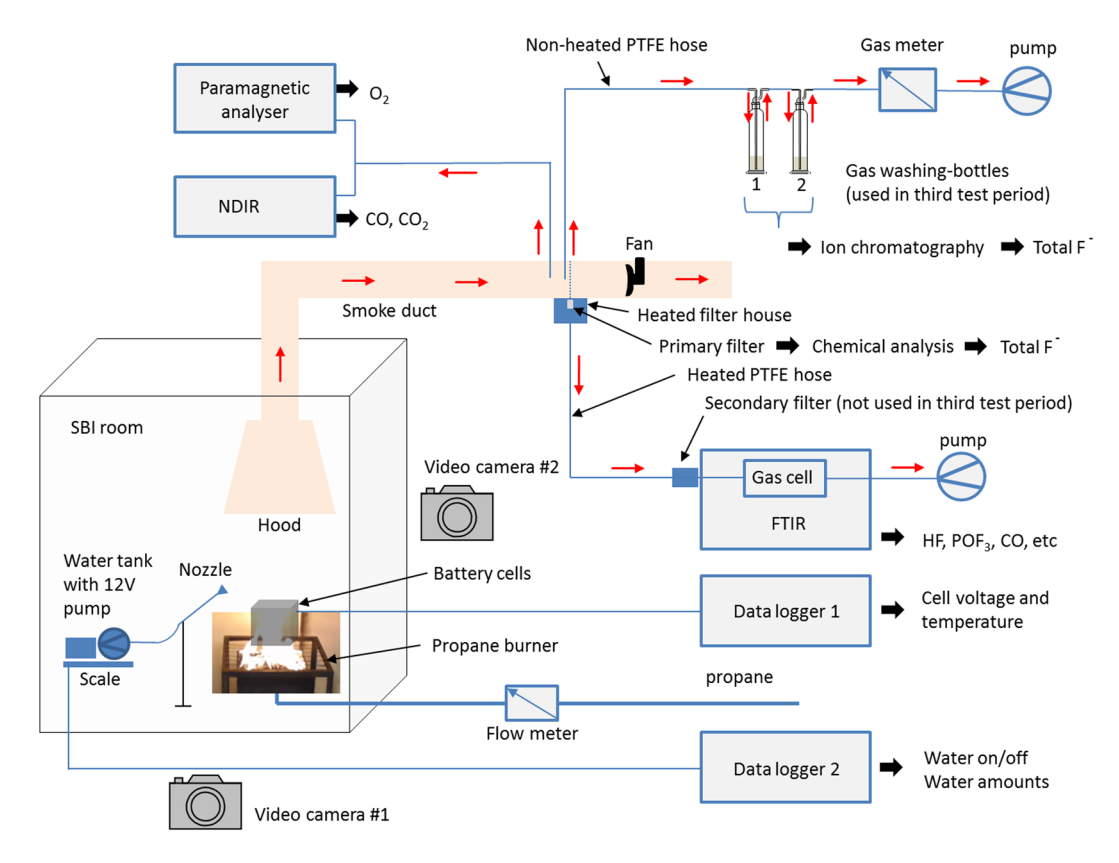


Figure 7. Schematic illustration of the experimental setup.

	Number of tests per SOC-level					
Battery	0%	25%	50%	75%	100%	Number of tests
A	1+1*	1	3+4*	1	3+3*	17
В	1	1	1	1	3+1*	8
С	1	1	3	1	2+1*	9
D			1		1	2
Е					1	1
F					1	1
G					1	1
Total number of tests						39

Table 4. Detailed test matrix of the fire tests. *repetition includes a variant, e.g. water mist or 2×5 -cell-pack (for battery type A).

The selected SOC level in each test was set using a charge/discharge procedure using ordinary laboratory equipment as well as dedicated battery test equipment, i.e. a *Digatron battery tester* and *Metrohm Autolab PGSTAT302N* with 20 A booster module. The cells were first fully charged by constant current followed by constant voltage (CC-CV) according to the manufacturer's instructions. For cells intended for tests with less than 100% SOC, the cell was discharged to the selected SOC level, using constant discharge current (CC). A relative low current rate, about C/5, was used and voltage and current rates were within the manufacturer limits. In most cases each battery type was tested during the same test period. However, the tests for type C and D were split in several test periods, for type C repetitions on 50% SOC were conducted in all three test periods, and for type B repetitions at 100% SOC were made in two test periods, the latter one included a water mist test.

All batteries were unused and the calendar life time of the cells before the tests were approximately 6–12 months for type A, F and G and between approximately 2–3 years for type B-E. The pouch cells; type B, C and F was mechanically tied together with steel wires (0.8 mm diameter). The type A hard prismatic cells were tight together in packs of five cells, "5-cell-pack", using steel straps (1×13 mm). The hard prismatic and cylindrical cells were placed in boxes to protect test personnel from potential projectile hazards in case of cell explosions due to excessive pressure. The 5-cell-pack of type A was placed standing up, with the cell safety vents releasing straight upright in direction to the hood and smoke duct, inside a custom-made steel-net-box, see Fig. 8. Additionally, the 5-cell-pack of type A was fastened to the bottom of the steel-net-box with steel wire (0.8 mm diameter) in the

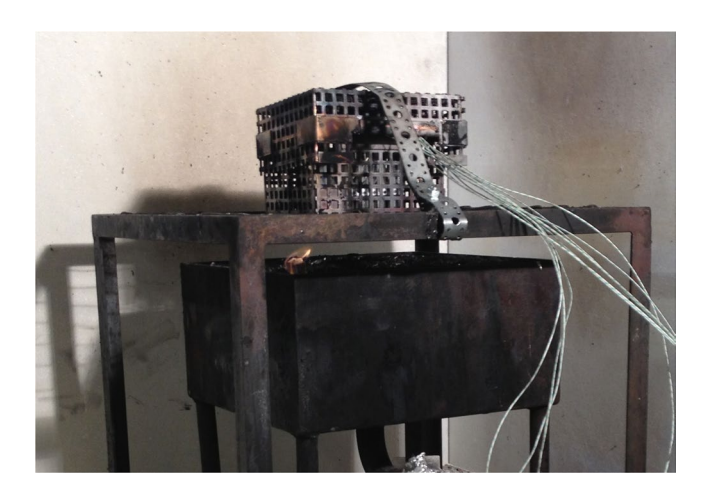


Figure 8. Photo of test type A, showing the 5-cell-pack inside a steel-net-box placed on the wire gratings. The sand bed for the propane burner is underneath the wire grating, a pilot flame (seen in front left corner of the burner) is used to ignite the propane gas.

corners to avoid it moving around due to e.g. explosion/rupture/venting. Type D and E cells were placed standing up in custom-made boxes made of non-combustible silica board and steel net at the top and bottom. Type G was placed in a steel net. The protective boxes and steel net were fastened in the wire gratings with steel wire and steel straps to avoid movement due to response to the fire. Care was taken to avoid external short circuiting when placing the battery on the wire gratings as well as avoiding accidental external electrical inter-cell-connections, e.g. for pouch cells the electrical tab terminals were cut. Still the battery test setup allowed that the separators and electrical insulation in the cells could melt due to the heat exposure which could cause various internal and external electrical contacts.

The battery surface temperature was measured with several type K thermocouples; the number of sensors varied for the different battery types. Battery cell surface temperature values presented in this paper are average values over the cell. Cell voltages were measured for type A, B, C and F battery tests. Cell voltage and thermocouple readings was sampled with 1 Hz using two types of data loggers, *Agilent 34972 A using an Agilent 34902 A reed multiplexer module* (for the third test period) and *Pico Technology ADC-24* (for the first and second test period).

Test procedure. The propane burner was started 2 minutes into each test, as indicated with arrows in the result figures in the paper. The burner was active as long as there was a heat contribution from the burning batteries; therefore, the burner was active for different durations of time for different batteries and SOC-levels. When the heat release from the batteries was no longer detectable, the power of the propane burner was doubled, i.e. to 32 kW, in order to be sure to fully burn out any residues of the batteries, for increased personnel safety. The fire emissions were collected in the hood and transferred in the smoke duct having a ventilation flow of $0.4 \, \text{m}^3$ /s, with the exception that $0.6 \, \text{m}^3$ /s was used in two tests with 100% SOC for type C. For these cases the values were scaled down to the lower flow values making the results from the two flow rates comparable. The SBI-room, see Fig. 7, had a ventilation inlet from an adjacent indoor laboratory hall (which had fresh air inlet from the ventilation system in the building), supplying ambient air with temperature about 20 °C entering beneath the propane burner. We consider the amount of ambient air to be sufficient to provide an oxygen-rich environment and thereby consider the battery fire as well-ventilated. However for some tests, during the rapid and energetic gas outbursts, a full combustion might not have occurred in these short time periods.

All tests were video recorded and for the majority of the tests an additional camera was used set at 90 degree angle from the other video camera, allowing simultaneous recording from two sides of the battery fire.

A part of the smoke duct flow was sampled to a Servomex 4100 Gas purity analyser where the oxygen content was measured by a paramagnetic analyser and CO and CO₂ were measured by a non-dispersive infrared sensor (NDIR). By combing these two measurements, the heat release rate (HRR) is calculated using the oxygen consumption method corrected by $\mathrm{CO_2}^{54}$. Each test day started with a blank test, i.e. using only the propane burner, to measure the HRR of the burner alone and measure blanks for FTIR and gas-washing bottles. In the presented HRR values of the battery tests the burner contribution to the HRR (about 16 kW, with slight daily variations, established by the blank tests) has been subtracted. The combined expanded uncertainty is ±5 kW for the HRR-values. By integrating the HRR values over the entire test, subtracting the HRR from the burner, the total heat release (THR) from the battery cells could be established. The oxygen consumption method is common in fire calorimetry, however when using it with batteries, the joule heating from electrical discharge within the cells is not accounted for, therefore the values of HRR and THR do not include the Joule heating. During the external fire tests, it is difficult to measure how much a battery cell is electrically discharged when the separator is melting. The energy ratios presented in Fig. 2b do not include any Joule heating as clearly stated by its definition. For 0% SOC the influence from Joule heating is in principle zero, however small amounts of joule heating might possibly be liberated when going to zero voltage even though other processes might occur. Li-ion cells can also release oxygen during thermal runaway and this could affect the measured O_2 levels. The amount of oxygen release varies

Spectral bands (cm ⁻¹)	Type of band		
POF ₃			
868-874	P-F symmetric stretching mode ²⁰		
1413-1418	P-O stretching mode ²⁰		
HF			
4172-4175	HF R-branch stretching mode ⁵⁸		
4202-4203	HF R-branch stretching mode ⁵⁸		

Table 5. FTIR spectral band used for measurements of POF₃ and HF.

for different electrode materials, e.g. LFP typically releases less oxygen than LCO. However, the ventilation flow is large and the O_2 released from the battery cells is regarded as negligible.

Gas measurements. Besides the gas measurements in the SBI apparatus, measurements of gases were also conducted by online Fourier transform infrared spectroscopy (FTIR). The FTIR offers broad and diverse spectra of gases, the focus was however on fluoride gas emissions. The FTIR used was a *Thermo Scientific Antaris IGS analyzer (Nicolet)* with a gas cell. The gas cell was heated to $180\,^{\circ}$ C and had a volume of $0.2\,L$, $2.0\,\mathrm{m}$ path length and a cell pressure of $86.7\,\mathrm{kPa}$ which was maintained during the tests. The spectral resolution of the FTIR was $0.5\,\mathrm{cm}^{-1}$ (accuracy $0.01\,\mathrm{cm}^{-1}$) and $10\,\mathrm{scans}$ where used to collect a spectrum every $12\,\mathrm{s}$, giving both accurate intensity, as well as relatively rapid measurements with its five spectrum per minute rate. A part of the duct flow, taken along the full duct pipe width (in the mid height of the pipe) from around $15\,\mathrm{sampling}$ holes (about 2 mm diameter, directed opposite to flow, pipe end was closed), was taken to online FTIR measurement. This sub-flow was extracted through a primary filter inside a heated filter house ($180\,^{\circ}\mathrm{C}$) and then extracted through an $8.5\,\mathrm{m}$ sampling PTFE hose, heated to $180\,^{\circ}\mathrm{C}$, and then through a secondary filter and finally through the gas cell of the FTIR. The sub-flow was selected to be $3.5\,\mathrm{L/min}$ using a pump located after the FTIR gas cell. Between each test the FTIR sampling system was flushed with N_2 gas and a new background spectrum was measured. There is a natural delay time between the FTIR and the heat release measurement. In order to time synchronize them the (CO_2 measurements from both the FTIR and the NDIR) part of the heat release rate measurement, were overlayed.

One primary filter (M&C ceramic filter, type "F-2K") was used per test and was chemically analysed for fluoride content after the test. It is known that HF may be partly adsorbed by this type of filter 56. The fluoride amount absorbed by the filter was determined by leaching the filter in an ultrasonic water bath for at least 10 min and thereafter the fluoride content in the water was measured by ion chromatography with a conductive detector, according to the method B.1 (b) of the SS-ISO 19702:2006 Annex B standard. The amount of HF is calculated by assuming that all fluoride ions present in the filter derives from HF. The secondary filter (M&C sintered steel filter), heated to 180 °C, was the same in all tests in the first and second test period. In the third test period the secondary filter was removed in order to decrease delay time and losses. The third test period started with burning 10 cells of type A in order to saturate the FTIR sampling system with HF and it was conducted because in the first and the second test period the first tests had indicated low HF values, HF was potentially lost during saturation of the gas collecting system.

The FTIR was calibrated^{29,57} for HF and POF₃. The minimum detection limit (MDL) for HF was 1.7 ppm and the limit of quantification (LOQ) was established to 5.7 ppm. The detection limit for POF₃ was 6 ppm²⁹. PF₅ was also qualitatively detectable by the FTIR²⁹ but not quantitatively calibrated. A classical least square (CLS) method was used for the quantification of HF and POF₃ using the spectral bands specified in Table 5. The relative error of the HF prediction is lower than 10 rel-%.

For all measurements, except type G, the measured ppm levels of HF were above the detection level. For POF₃, the maximum concentration was 11 ppm (5-cells) and 19 ppm (10-cells).

When the FTIR measurement stopped, HF levels were, in some of the tests, still somewhat above the detection limit, even though no HRR contribution was measured from the batteries. It is also possible that the HF was temporarily clogged in the sampling system. Some HF might not have been collected in the measurements and the effect of this error is largest for the batteries that give the lowest values. Thus the reported values might underestimate the released gas emissions.

In order to further improve the accuracy of the FTIR measurements, a data offset determination and a subsequent adjustment of the HF values was performed. The improvement was greatest for tests with lower concentrations, closer to the MDL value, e.g. type A with 5 cells with low values during relatively short periods of time. With 10 cells per test, the type A batteries gave higher signal-to-noise levels. The FTIR measurements started around 8 minutes before the burner was started. The calculated average HF ppm noise level was treated as an offset that had both negative and positive values, ranging from extreme values of about -2 to 3.5 ppm. This offset was compensated for by assuming a constant offset value and adding positive or negative offset values to the total HF release value. Note that the reported concentration values in ppm are only valid for the measurements in the smoke duct of our specific test equipment and method. The HF and POF3 concentration values (in ppm) were used for calculating the corresponding production rates (in mg/s) using the ideal gas law and taking into account the measured ventilation flow rate in the smoke duct.

In the third test period the total amounts of water soluble fluorides were determined using gas-washing bottle technique. This was made in order to validate the results from the FTIR measurements with a separate measurement technique. The water soluble fluorides were collected in the bottles and the amount of HF was calculated by assuming that all fluoride ions present derives from HF. The sample gas was extracted from the center of

the smoke duct using a non-heated 6 mm (o.d.) diameter PTFE sampling tube with a length of about 1.5 m. The sampling was made using two gas-washing bottles connected in series each containing $40\,\mathrm{mL}$ of an alkaline buffer solution ($20\,\mathrm{mM}$ Na $_2\mathrm{CO}_3/20\,\mathrm{mM}$ NaHCO $_3$). The second bottle was used to capture any losses from the first bottle. The sampling flow was 1.0 normal-L/min and the total sampled volume during a test was measured by a calibrated gas volume meter. The sampling flow rate was checked before the start of each test using a *Gilian Gilibrator-2 NIOSH Primary Standard Air Flow Calibrator* gas flow meter. The procedure during a test was to continuously sample during the full test time. When the test was completed, the sampling tube was disconnected from the exhaust duct to allow rinsing of the tube with buffer solution, about 30 mL in the first gas-washing bottle, to collect any fluoride deposited on the inner walls of the tubing, in order to minimize losses in the tube. Since the tube was rinsed, heating of the tube was not necessary (any condensation in tube was collected anyhow). Analysis of fluorine content of the absorption solutions was made using High Performance Ion Chromatography (HPIC). The contents of the two gas-washing bottles were analyzed separately. The bottles were rinsed with distilled water between each test in order to minimize any interference between tests.

Water mist test. In the water mist tests, a custom-made equipment was constructed, including a 12 V automotive pump and water container which was placed on a scale measuring the weight of the water. The scale readings and the on/off manual switching (of the 12 V) was recorded with 1 Hz using *Pico Technology ADC-24* with a custom-made *LabVIEW* program. The water mist was sprayed on or above the batteries using a metal nozzle. In order for precise time synchronization, the on/off 12 V signal was recorded by both data loggers (data logger 1 and data logger 2). A blank test, i.e. using only the propane burner and without batteries, was performed in order to calibrate the setup. The water flow was around 190 g water per min and consisted of deionized water.

References

- 1. Samsung Note 7: Press Conference Details, Samsung US, Our safety promise, http://www.samsung.com/us/explore/committed-to-quality/?CID = van-brd-brd-0119-10000141, Date of access: 06/04/2017.
- Prigg, M. Nasa reveals shocking video of secretive military 'RoboSimian' EXPLODING as its batteries catch fire (2016), http://www.dailymail.co.uk/sciencetech/article-3883158/Nasa-reveals-shocking-video-secretive-military-RoboSimian-EXPLODING-batteries-catch-fire.html, Date of access: 06/04/2017.
- 3. Aircraft Serious Incident Investigation Report, JA804A. Japan Transport Safety Board (2014), Available online: http://www.mlit.go.jp/jtsb/eng-air_report/JA804A.pdf, Date of access: 13/02/2017.
- Auxiliary Power Unit Battery Fire, Japan Airlines Boeing 787–8, JA829J, Boston, Massachusetts; NTSB/AIR-14/01. National Transportation Safety Board (2014), Available online: http://www.ntsb.gov/investigations/AccidentReports/Reports/AIR1401.pdf, Date of access: 13/02/2017.
- Chevrolet Volt battery incident overview report, National Highway Traffic Safety Administration (NHTSA), DOT HS 811 573
 (2012).
- Doughty, D. & Roth, E. P. A general discussion of Li ion battery safety. The Electrochem. Soc. Interface, summer 2012, 37–44 (2012).
- 7. Larsson, F. & Mellander, B.-E. Abuse by external heating, overcharge and short circuiting of commercial lithium-ion battery cells. *J. of The Electrochem. Soc.* **161**(10), A1611–A1617 (2014).
- 8. Larsson, F., Andersson, P. & Mellander, B.-E. Are electric vehicles safer than combustion engine vehicles? in *Systems perspectives on* Electromobility (eds. Sandén, B. & Wallgren, P.) 33–44 (Chalmers University of Technology, 2014).
- 9. Finegan, D. P. *et al.* In-operando high-speed tomography of lithium-ion batteries during thermal runaway. *Nat. Commun.* **6**, 6924 (2015).
- 10. Larsson, F., Andersson, P. & Mellander, B.-E. Lithium-ion battery aspects on fires in electrified vehicles on the basis of experimental abuse tests. *Batteries* 2, 9 (2016).
- 11. Lopez, F. L., Jeevarajan, J. A. & Mukherjee, P. P. Experimental analysis of thermal runaway and propagation in lithium-ion battery modules. *J. of The Electrochem. Soc* **162**(9), A1905–A1915 (2015).
- 12. Lamb, J., Orendorff, C. J., Steele, L. A. M. & Spangler, S. W. Failure propagation in multi-cell lithium-ion batteries. *J. of Power Sources* 283, 517–523 (2015).
- 13. Larsson, F., Anderson, J., Andersson, P. & Mellander, B.-E. Thermal modelling of cell-to-cell fire propagation and cascading thermal runaway failure effects for lithium-ion battery cells and modules using fire walls. *J. of The Electrochem. Soc.* **163**(14), A2854–A2865 (2016)
- Lebedeva, N. P. & Boon-Brettz, L. Considerations on the chemical toxicity of contemporary Li-ion battery electrolytes and their components. J. of The Electrochem. Soc. 163(6), A821–A830 (2016).
- 15. Sun, J. et al. Toxicity, a serious concern of thermal runaway from commercial Li-ion battery. Nano Energy 27, 313-319 (2016).
- 16. Nedjalkov, A. *et al.* Toxic gas emissions from damaged lithium ion batteries–analysis and safety enhancement solution. *Batteries* 2, 5 (2016).
- 17. Liu, K. et al. Electrospun core-shell microfiber separator with thermal-triggered flame-retardant properties for lithium-ion batteries. Sci. Adv. 3, e1601978 (2017).
- 18. Park, Y.-U. et al. Tailoring a fluorophosphate as a novel 4 V cathode for lithium-ion batteries. Scientific Reports 2, 704 (2012).
- 19. Ortiz, G. F. et al. Enhancing the energy density of safer Li-ion batteries by combining high-voltage lithium cobalt fluorophosphate cathodes and nanostructured titania anodes. Scientific Reports 6, 20656 (2016).
- Yang, H., Zhuang, G. V. & Ross Jr, P. Thermal stability of LiPF₆ salt and Li-ion battery electrolytes containing LiPF₆. J. of Power Sources 161, 573–579 (2006).
- 21. Kawamura, T., Okada, S. & Yamaki, J.-i Decomposition reaction of LiPF₆-based electrolytes for lithium ion cells. *J. of Power Sources* **156**, 547–554 (2006).
- 22. Documentation for immediately dangerous to life or health concentrations (IDLHs) for hydrogen fluoride (as F). *The National Institute for Occupational Safety and Health (NOISH)* (1994).
- 23. Acute exposure guideline levels for selected airborne chemicals: volume 4, subcommittee on acute exposure guideline levels. ISBN: 0-309-53013-X. Committee on Toxicology, National Research Council (2004).
- 24. Middelman, A. Hygiensiska gränsvärden AFS 2015:7, Hygieniska gränsvärden. Arbetsmiljöverkets föreskrifter om hygieniska gränsvärden och allmänna råd om tillämpningen av föreskrifterna. ISBN 978-91-7930-628-1. ISSN 1650-3163. Swedish Work Environment Authority (2015).
- 25. Guéguen, A. et al. Decomposition of LiPF₆ in high energy lithium-ion batteries studied with online electrochemical mass spectrometry. J. of The Electrochem. Soc. 163(6), A1095–A1100 (2016).

- Chatelain, M. D. & Adams, T. E. Lithium ion gas sampling of vented cells. Proceedings of the Power Sources Conference 42, 87–89 (2006).
- 27. Blum, A. F. & Long Jr, R. T. Hazard assessment of lithium ion battery energy storage systems. Fire Protection Research Foundation (2016).
- Larsson, F., Andersson, P., Blomqvist, P., Lorén, A. & Mellander, B.-E. Characteristics of lithium-ion batteries during fire tests. J. of Power Sources 271, 414–420 (2014).
- 29. Larsson, F., Andersson, P., Blomqvist, P. & Mellander, B.-E. Gas emissions from Lithium-ion battery cells undergoing abuse from external fire in *Conference proceedings of Fires in vehicles* (FIVE) 2016 (eds. Andersson, P. & Sundstrom, B.) 253–256 (SP Technical Research Institute of Sweden, 2016).
- 30. Ribière, P. *et al.* Investigation on the fire-induced hazards of Li-ion battery cells by fire calorimetry. *Energy Environ. Sci.* **5**, 5271–5280 (2012).
- 31. Lecocq, A. Scenario-based prediction of Li-ion batteries fire-induced toxicity. J. of Power Sources 316, 197-206 (2016).
- 32. Lecocq, A., Bertana, M., Truchot, B. & Marlair, G. Comparison of the fire consequences of an electric vehicle and an internal combustion engine vehicle in *Conference proceedings of Fires in vehicles* (FIVE) 2012 (eds. Andersson, P. & Sundstrom, B.) 183–193 (SP Technical Research Institute of Sweden, 2012).
- 33. Ohsaki, T. et al. Overcharge reaction of lithium-ion batteries. J. of Power Source 146, 97-100 (2005).
- 34. Abraham, D. P. et al. Diagnostic examination of thermally abused high-power lithium-ion cells. J. of Power Sources 161, 648–657 (2006).
- 35. Roth, E. P. Abuse response of 18650 Li-ion cells with different cathodes using EC:EMC/LiPF₆ and EC:PC:DMC/LiPF₆ electrolytes. ECS Transactions 11(19), 19–41 (2008).
- 36. Golubkov, A. W. et al. Thermal-runaway experiments on consumer Li-ion batteries with metal-oxide and olivin-type cathodes. RSC Adv. 4, 3633–3642 (2014).
- 37. Golubkov, A. W. et al. Thermal runaway of commercial 18650 Li-ion batteries with LFP and NCA cathodes—impact of state of charge and overcharge. RSC Adv. 5, 57171–57186 (2015).
- Spinner, N. S. et al. Physical and chemical analysis of lithium-ion battery cell-to-cell failure events inside custom fire chamber. J. of Power Sources 279, 713–721 (2015).
- 39. Fu, Y. et al. An experimental study on burning behaviors of 18650 lithium ion batteries using a cone calorimeter. J. of Power Sources 273, 216–222 (2015).
- 40. Huang, P., Wang, Q., Li, K., Ping, P. & Sun, J. The combustion behavior of large scale lithium titanate battery. *Scientific Reports* 5, 7788 (2015).
- 41. Ping, P. *et al.* Study of the fire behavior of high-energy lithium-ion batteries with full-scale burning test. *J. of Power Sources* **285**, 80–89 (2015).
- 42. Roth, E. P. & Orendorff, C. J. How electrolytes influence battery safety. The Electrochem. Soc. Interface, summer 2012, 45-49 (2012).
- 43. Eshetu, G. G. et al. In-depth safety-focused analysis of solvents used in electrolytes for large scale lithium ion batteries. Phys. Chem. Chem. Phys. 15, 9145–9155 (2013).
- 44. Lamb, J., Orendorff, C. J., Roth, E. P. & Langendorf, J. Studies on the thermal breakdown of common Li-ion battery electrolyte components. J. of The Electrochem. Soc. 162(10), A2131–A2135 (2015).
- 45. Eshetu, G. G. et al. Fire behavior of carbonates-based electrolytes used in Li-ion rechargeable batteries with a focus on the role of the LiPF₆ and LiFSI salts. J. of Power Sources 269, 804–811 (2014).
- 46. Andersson, P., Blomqvist, P., Lorén, A. & Larsson, F. Using Fourier transform infrared spectroscopy to determine toxic gases in fires with lithium-ion batteries. *Fire and Materials* 40(8), 999–1015 (2016).
- 47. Lux, S. F. The mechanism of HF formation in LiPF₆ based organic carbonate electrolytes. *Electrochem. Comm.* 14, 47-50 (2012).
- 48. Lux, S. F., Chevalier, J., Lucas, I. T. & Kostecki, R. HF formation in LiPF₆-based organic carbonate electrolytes. *ECS Electrochem. Lett.* 2(12), A121–A123 (2013).
- 49. Wilken, S., Treskow, M., Scheers, S., Johansson, P. & Jacobsson, P. Initial stages of thermal decomposition of LiPF₆-based lithium ion battery electrolytes by detailed Raman and NMR spectroscopy. *RSC Adv.* 3, 16359–16364 (2013).
- 50. Hammami, A., Raymond, N. & Armand, M. Runaway risk of forming toxic compounds. Nat. 424, 635-636 (2013).
- 51. Campion, C. L. et al. Suppression of toxic compounds produced in the decomposition of lithium-ion battery electrolytes. Electrochem. and Solid-State Lett. 7(7), A194-A197 (2004).
- 52. Liu, X. et al. Heat release during thermally-induced failure of a lithium ion battery: impact of cathode composition. Fire Safety Journal 85, 10–22 (2016).
- 53. Lyon, R. E. & Walters, R. N. Energetics of lithium ion battery failure. J. of hazardous materials 318, 164-172 (2016).
- 54. EN 13823:2010. Reaction to fire tests for building products -building products excluding floorings exposed to the thermal attack by a single burning item. *European Committee for Standardization* (2010).
- 55. EN 13501-1:2007 + A1:2009. Fire classification of construction products and building elements part 1: classification using data from reaction to fire tests. *European Committee for Standardization* (2009).
- 56. ISO 19702:2006. Toxicity testing of fire effluents–guidance for analysis of gases and vapours in fire effluents using FTIR gas analysis. *International Organization for Standardization* (2006).
- 57. Andersson, P., Blomqvist, P., Lorén, A. & Larsson, F. Investigation of fire emissions from Li-ion batteries. SP Technical Research Institute of Sweden. SP Report 2013:5 (2013).
- 58. Hollas, J. M. Modern Spectroscopy, 3ed. (John Wiley & Sons, 1996).

Acknowledgements

The Swedish Energy Agency and its FFI-program, and Carl Tryggers Stiftelse för Vetenskaplig Forskning are acknowledged for their financial support. Several persons at RISE Research Institutes of Sweden and Chalmers University of Technology have been involved in this work and are gratefully acknowledged.

Author Contributions

F. Larsson planned the experiments, partially together with P. Andersson and B.-E. Mellander. P. Andersson made the initial data process of the SBI heat release data. P. Blomqvist planned and performed the FTIR and gas-washing bottles measurements and made the initial data processing. F. Larsson prepared the batteries and performed the measurement and data analyses of temperature, cell voltage and water mist, and did the post-measurements and final data processing. Water mist setup was planned and constructed by B.-E. Mellander and F. Larsson. All four authors were involved in the analyses of the data and wrote the paper.

Additional Information

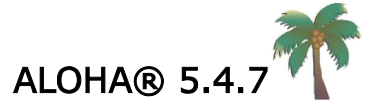
Competing Interests: The authors declare that they have no competing interests.

Publisher's note: Springer Nature remains neutral with regard to jurisdictional claims in published maps and institutional affiliations.

Open Access This article is licensed under a Creative Commons Attribution 4.0 International License, which permits use, sharing, adaptation, distribution and reproduction in any medium or format, as long as you give appropriate credit to the original author(s) and the source, provide a link to the Creative Commons license, and indicate if changes were made. The images or other third party material in this article are included in the article's Creative Commons license, unless indicated otherwise in a credit line to the material. If material is not included in the article's Creative Commons license and your intended use is not permitted by statutory regulation or exceeds the permitted use, you will need to obtain permission directly from the copyright holder. To view a copy of this license, visit https://creativecommons.org/licenses/by/4.0/.

© The Author(s) 2017

ATTACHMENT 7 AIR DISPERSION MODELING RESULTS OF AN HF RELEASE EVENT IN ACTON.



Time: December 6, 2023 1325 hours PST (using computer's clock)

Chemical Name: HYDROGEN FLUORIDE

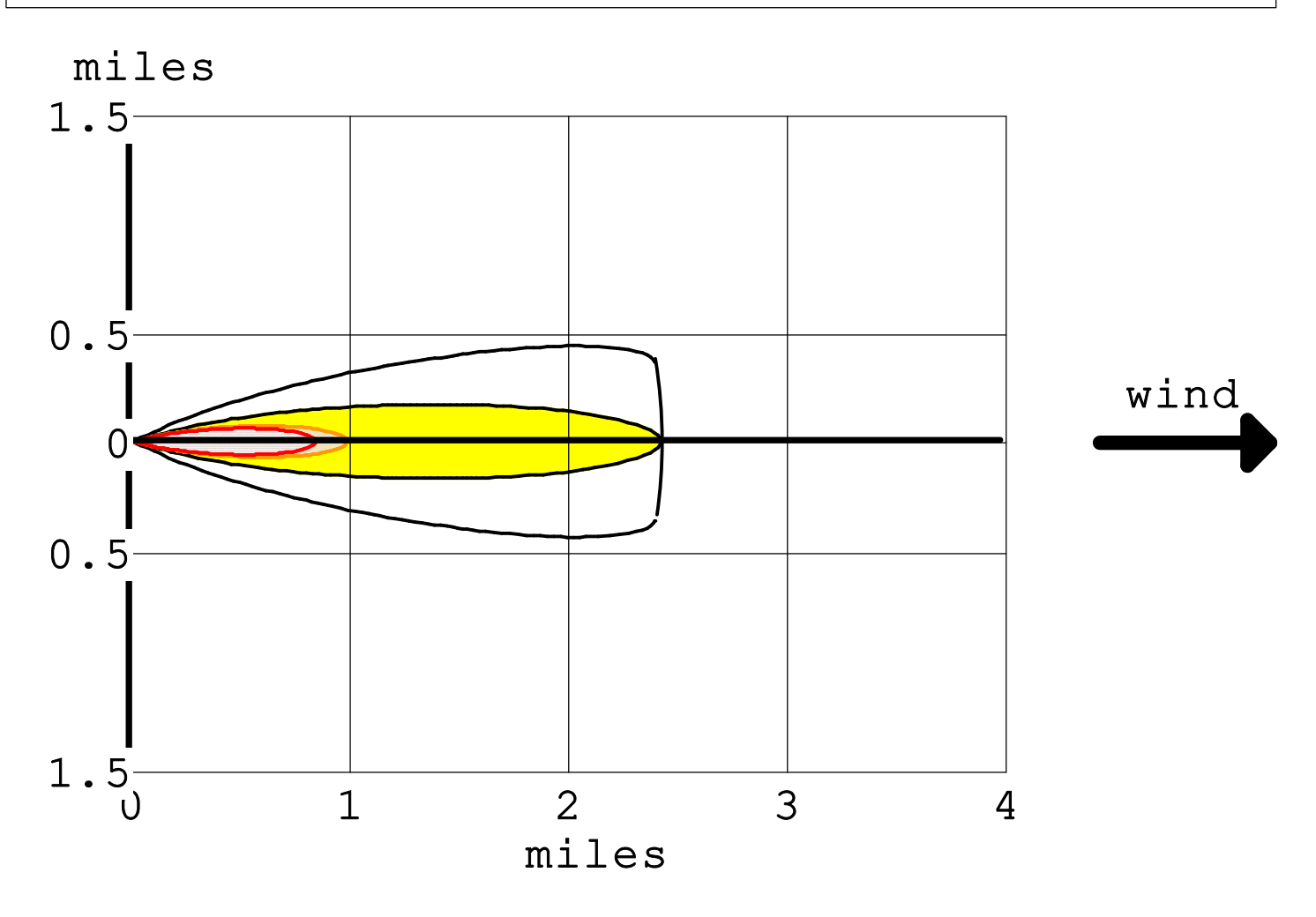
Warning: HYDROGEN FLUORIDE can react with water and/or water vapor. This can affect the evaporation rate and downwind dispersion. ALOHA cannot accurately predict the air hazard if this substance comes in contact with water.

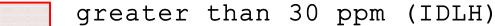
Wind: 10 miles/hour from 270° true at 5 meters

THREAT ZONE: (GAUSSIAN SELECTED)

Model Run: Gaussian

Red : 1491 yards --- (30 ppm = IDLH)
Orange: 1750 yards --- (20 ppm = ERPG-2)
Yellow: 2.4 miles --- (2 ppm = ERPG-1)





greater than 20 ppm (ERPG-2)

greater than 2 ppm (ERPG-1)

— wind direction confidence lines



SITE DATA: Location: ACTON, CALIFORNIA

Building Air Exchanges Per Hour: 0.89 (unsheltered single storied) Time: December 6, 2023 1325 hours PST (using computer's clock)

CHEMICAL DATA:

Warning: HYDROGEN FLUORIDE can react with water and/or water vapor. can affect the evaporation rate and downwind dispersion. ALOHA cannot accurately predict the air hazard if this substance comes in contact with

Chemical Name: HYDROGEN FLUORIDE

CAS Number: 7664-39-3 Molecular Weight: 20.01 g/mol

AEGL-1 (60 min): 1 ppm AEGL-2 (60 min): 24 ppm AEGL-3 (60 min): 44 ppm

IDLH: 30 ppm

Ambient Boiling Point: 61.8° F

Vapor Pressure at Ambient Temperature: greater than 1 atm Ambient Saturation Concentration: 1,000,000 ppm or 100.0%

ATMOSPHERIC DATA: (MANUAL INPUT OF DATA)

Wind: 10 miles/hour from 270° true at 5 meters

Ground Roughness: open country Cloud Cover: 0 tenths Air Temperature: 85° F Stability Class: D No Inversion Height Relative Humidity: 5%

SOURCE STRENGTH:

Direct Source: 152 kilograms/min Source Height: 8 feet

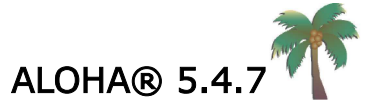
Release Duration: 1 minute Release Rate: 5.59 pounds/sec Total Amount Released: 335 pounds

Note: This chemical may flash boil and/or result in two phase flow. Use both dispersion modules to investigate its potential behavior.

THREAT ZONE: (GAUSSIAN SELECTED)

Model Run: Gaussian

Red : 1491 yards --- (30 ppm = IDLH) Orange: 1750 yards --- (20 ppm = ERPG-2)Yellow: 2.4 miles --- (2 ppm = ERPG-1)



Time: December 6, 2023 1325 hours PST (using computer's clock)

Chemical Name: HYDROGEN FLUORIDE

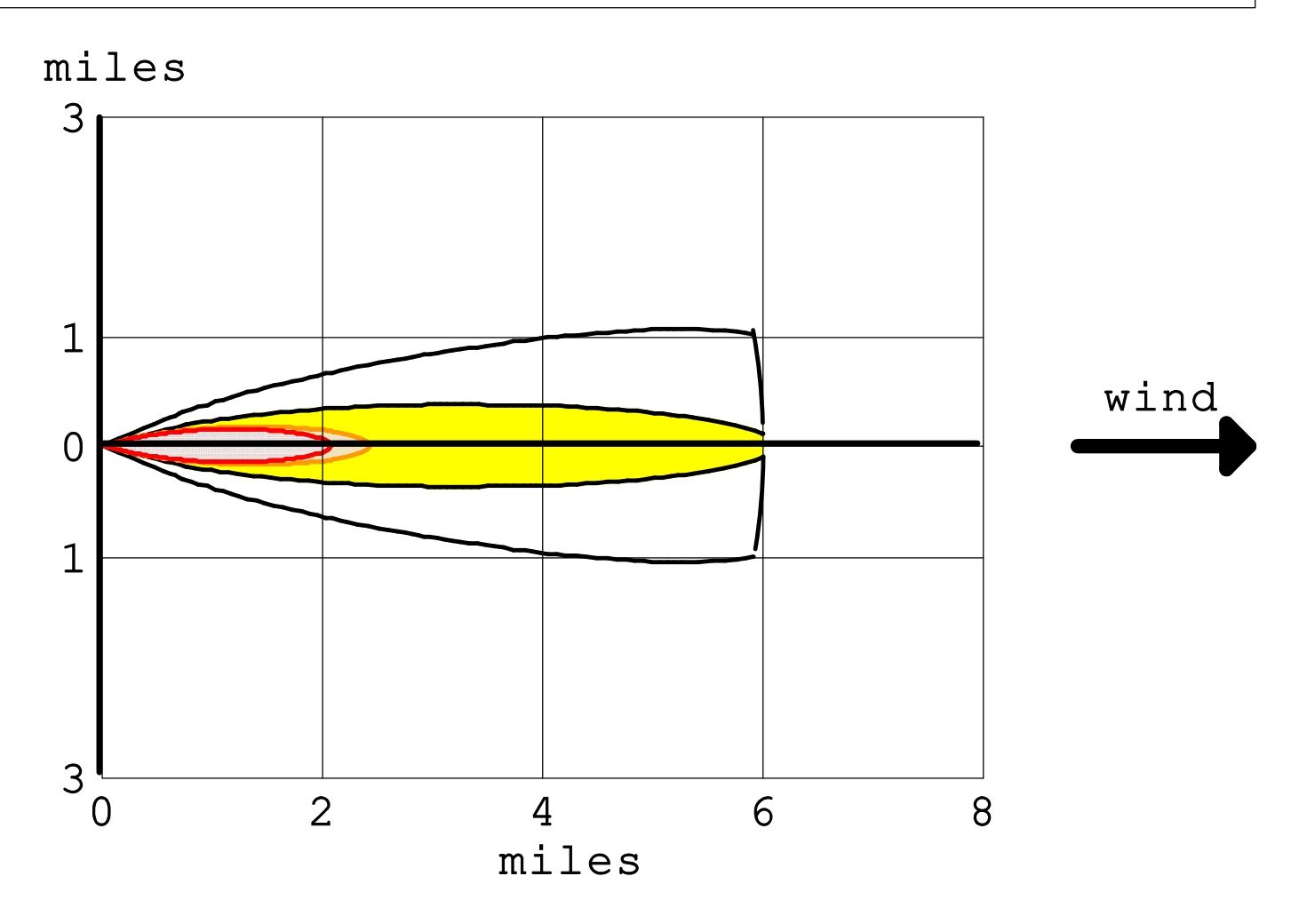
Warning: HYDROGEN FLUORIDE can react with water and/or water vapor. This can affect the evaporation rate and downwind dispersion. ALOHA cannot accurately predict the air hazard if this substance comes in contact with water.

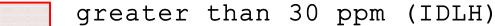
Wind: 10 miles/hour from 270° true at 5 meters

THREAT ZONE: (GAUSSIAN SELECTED)

Model Run: Gaussian

Red : 2.1 miles --- (30 ppm = IDLH)
Orange: 2.4 miles --- (20 ppm = ERPG-2)
Yellow: 6.1 miles --- (2 ppm = ERPG-1)





greater than 20 ppm (ERPG-2)

greater than 2 ppm (ERPG-1)

wind direction confidence lines



```
SITE DATA:
  Location: ACTON, CALIFORNIA
  Building Air Exchanges Per Hour: 0.89 (unsheltered single storied)
  Time: December 6, 2023 1325 hours PST (using computer's clock)
CHEMICAL DATA:
  Warning: HYDROGEN FLUORIDE can react with water and/or water vapor.
  can affect the evaporation rate and downwind dispersion. ALOHA cannot
  accurately predict the air hazard if this substance comes in contact with
  Chemical Name: HYDROGEN FLUORIDE
  CAS Number: 7664-39-3
                                         Molecular Weight: 20.01 g/mol
  AEGL-1 (60 min): 1 ppm AEGL-2 (60 min): 24 ppm
                                                      AEGL-3 (60 min): 44 ppm
  IDLH: 30 ppm
  Ambient Boiling Point: 61.8° F
  Vapor Pressure at Ambient Temperature: greater than 1 atm
  Ambient Saturation Concentration: 1,000,000 ppm or 100.0%
ATMOSPHERIC DATA: (MANUAL INPUT OF DATA)
  Wind: 10 miles/hour from 270° true at 5 meters
  Ground Roughness: open country
                                         Cloud Cover: 0 tenths
  Air Temperature: 85° F
                                         Stability Class: D
  No Inversion Height
                                         Relative Humidity: 5%
SOURCE STRENGTH:
  Direct Source: 1520 kilograms/min
                                         Source Height: 8 feet
  Release Duration: 1 minute
  Release Rate: 55.9 pounds/sec
  Total Amount Released: 3,351 pounds
  Note: This chemical may flash boil and/or result in two phase flow.
     Use both dispersion modules to investigate its potential behavior.
THREAT ZONE: (GAUSSIAN SELECTED)
  Model Run: Gaussian
      : 2.1 miles --- (30 ppm = IDLH)
  Orange: 2.4 miles --- (20 ppm = ERPG-2)
  Yellow: 6.1 \text{ miles } --- (2 \text{ ppm} = \text{ERPG}-1)
```